UNIVERSITY OF OKLAHOMA

GRADUATE COLLEGE

RISK-BASED EVALUATION AND MANAGEMENT OF CYBER-PHYSICAL-SOCIAL SYSTEMS DURING PANDEMIC CRISIS

A DISSERTATION

SUBMITTED TO THE GRADUATE FACULTY

in partial fulfillment of the requirements for the

Degree of

DOCTOR OF PHILOSOPHY

By

LEILI SOLTANISEHAT

Norman, Oklahoma

2022

RISK-BASED EVALUATION AND MANAGEMENT OF CYBER-PHYSICAL-SOCIAL SYSTEMS DURING PANDEMIC CRISIS

A DISSERTATION APPROVED FOR THE

SCHOOL OF INDUSTRIAL AND SYSTEMS ENGINEERING

BY THE COMMITTEE CONSISTING OF

Dr. Kash Barker, Chair

Dr. Andrés D. González

Dr. Yang Hong,

Dr. Theodore Trafalis

Dr. Rui Zhu

To:

Baba Gholamreza, my first role model and the light to the future

Maman Sakineh, my first angel of unconditional love

Khahar joon Azar, my wingless angel of hearts

Dadash Yaser, my pure love-full support

Abji Mozhgan, my lovely twin

for their continuous unconditional love, support, and sacrifices for me

&

Reza, my life's love

for his continuous mentorship, support, and love

Acknowledgments

This dissertation is a result of the continuous support, mentoring, and encouragement from several people involved in my academic life.

I express my gratitude to Professor Kash Barker for his continuous encouragement, support, and faith in me. He supported me during my challenging time two years ago, challenged me to go beyond my comfort zones, to believe in myself again, dare to step into the new research thrusts, and elevate my standards as a scholar. The fundamental principles embodied within the Risk-Based Systems Analytics Laboratory that is directed by Dr. Barker is to focus on scholarship and collaboration. As I reflect upon myself, I realize that I have significantly grown as a person both professionally and personally in the last years with Dr. Barker's research team.

Secondly, I want to thank my committee, Dr. Andres Gonzalez, Dr. Yang Hong, Dr. Theodore Trafalis, and Dr. Rui Zhu, for all of their feedback. A sincere gratitude to Dr. Gonzalez, for his continuous support and collaboration beyond the duties of committee members. A special thanks to Dr. Shivakumar Raman and Dr. Randa Shehab, who understood me in the challenging moments of my academic life and gave me the courage and support to continue.

I am very appreciative of my husband, Reza Alizadeh, who has been mentoring me during the last six years, taught me how to be a researcher with his patience, supported me during ups and downs, and pushed me out of my comfort zone.

Finally, I am also very appreciative of my friends Nafiseh, Ganeshvar, Safa, Bucket, and Deniz for their amazing support and encouragement as lab-mate.

TABLE OF CONTENTS

List of Tables

List of Figures

Abstract

This research focuses on risk-based evaluation and management of cyber-physical-social systems during a pandemic crisis. The ongoing novel coronavirus (COVID-19) epidemic has caused serious challenges for the world's countries. The health and economic crisis caused by the COVID-19 pandemic highlights the necessity for a deeper understanding and investigation of the best mitigation policy. While different control strategies in the early stages, such as lockdowns and school and business closures, have helped decrease the number of infections, these strategies have had an adverse economic impact on businesses and some controversial impacts on social justice. Therefore, optimal timing and scale of closure and reopening strategies are required to prevent both different waves of the pandemic and the negative socio-economic impact of control strategies. To maximize the effectiveness of the controlling policies during a major crisis like a pandemic, we propose two mathematical frameworks which optimize the contorting policy while considering three sets of important factors, including the epidemiologic, economic, and social impact of the pandemic. Each formulation quantifies the epidemiologic impact using a modified SIRD (susceptible-infected-recovered-deceased) model which captures the number of infected, recovered, immune, and deceased populations. The two formulations propose different approaches for measuring the social and economic impacts of the pandemic.

In the first formulation, the economic impact is a twofold measure, first the unmet demand because of supply perturbation (due to industry closure), and the second is the local business shrinkage because of demand perturbation (due to the state closure). The modified SIRD model is combined with a multi-commodity maximum network flow problem (MNFP) in which the unmet demand is measured in a network of states and industries. The proposed

formulation is implemented on a dataset that includes 11 states, the District of Columbia (including the states in New England and the mid-Atlantic), and 19 industries in the US.

In the second formulation, the economic impact is measured using the supply side multi-regional inoperability input-output model, accounting for the inoperability of each industry to satisfy the demand of final consumers and other industries, due to its closure. Also, the second formulation measures the social impact of the pandemic policy, by incorporating the vulnerability of social communities to get infected due to state opening or to lose their job due to the closure of the state. We test the efficacy of proposed formulations on the real data set of COVID-19 applicable to 50 states, the District of Columbia, and 19 industries.

Both formulations are multi-objective mixed integer programming with three objectives which are solved using the augmented ε-constraint approach. The final pandemic policy is selected from the set of Pareto-optimal solutions based on the least cubic distance of the solution from the optimal value of each objective. The Pareto-optimal solutions suggest that for any control decision (state and industry closure or reopening), the economic impact and the epidemiologic impact change in the opposite direction, and it is more effective to close most states while keeping the majority of industries open. For each Pareto optimal solution, the unmet demand and the propagation of inoperability to the industries and states can be tracked down. This will give a holistic view of the impact of the pandemic policy on the health, economy, and social justice aspects of the country.

Chapter 1: INTRODUCTION AND MOTIVATION

1.1. Overview

As of June 2022, more than 543 million cases of COVID-19 disease and 6.33 million deaths have been confirmed and reported in the world, with 86.9 million infected cases and 1.01 million deceased cases in the US. The pandemic has caused both a public health crisis and an economic crisis in the world. It threatened lives, disrupted the healthcare system by pushing hospitals and health centers to their capacity, and disrupted the economy by creating demand shock, supply shock, and financial shock (Bauer et al., 2020).

First, the pandemic crisis has had a different impact on various socio-demographic communities. The inequality in access to healthcare, occupations, education, and housing among others, put certain communities such as Black, Hispanic, and Native Americans in a more vulnerable situation. For example, Black and Native American use communities' public transit, which increases the infection rate. Also, Black and Hispanic populations live in dense urban area which has a higher rate of infection (Cowger et al., 2020).

Second, the un-organized social distancing and the quarantine policies caused a significant demand shock in some industries. While the lack of employees and business closure reduced the economy's capacity (Gupta et al., 2020). The disrupted supply and demand equilibrium decreased the GDP of different countries and slowed down the economy (Routley, 2020). COVID-19 pandemic and its associated shutdowns, also created an employment crisis, especially for the minor communities such as women, non-white workers, lower-wage workers, and less educated people (Stevenson, 2020). (Bauer et al., 2020)

summarized some of the early effects of COVID on the economy of the USA which include a 20% drop in small businesses revenue, a decrease in new business formation, increased Layoffs up to 10.1 million and increased shutdowns, increased absentees at work, increased job seekers up to 4.5 million, income shock in low-income families, increased food insecurity, among others.

While different control strategies in the early stages, such as lockdowns and school and business closures, and business closure, have helped with decreasing the number of infections, the adverse high economic impact on the businesses shows the necessity of a more comprehensive decision-making mechanism. More specifically, the optimal timing and scale of closure and reopening strategies are required to prevent both the pandemic's different waves and the negative social, economic and epidemiologic impact of control strategies.

1.2. Modeling the pandemic policy decisions

To model the pandemic policy, we focus on the two main decisions including the state closure and reopening and the industry closure and reopening. The closure of states and industries would lead to adverse economic consequences while decreasing the adverse epidemiological impacts and affecting social fairness. The economic impact is quantified as the unmet demand in each industry due to supply shock, the inoperability of the various industry due to the demand and supply shock, and the economic impact on local businesses due to lack of demand. The met/unmet demand of each state from the commodity of each industry at each time represents the inability of industries to satisfy the inter-industry and consumer demand at the state level, caused by policy-driven closure or by workforce

productivity losses due to the pandemic. The inoperability of each industry represents how the industry is dependent on the output of other industries over the nation and how any lack of supply or demand propagates to the economic system and affects various industries and states.

According to (Fairlie & Fossen, 2021), the pandemic and related social distancing, quarantine, and state closure policies have hurt different industries by shrinking the number of active businesses due to the shift in the demand for those industries. The drop in the number of active businesses causes a negative economic impact mainly by a higher unemployment rate. On the other hand, the increase in the negative epidemiological impact would result in workforce losses, leading to the inability of industries to have optimal productivity and may result in business closures. Since there is no reliable data available for such impact, the proposed model does not consider the later effect of the pandemic in the analysis.

The epidemiological impact in terms of the percentage of the infected population is measured based on the proposed modified dynamic SIRD model. The modified dynamic SIRD model represents the changes in four main population categories: infectious, susceptible, recovered/immune, and deceased individuals. It is assumed that the pandemic growth rate differs by state and industry, as the population density and the employment density vary by state and industry. More adverse epidemiological impacts result in more industry and state closures, while more substantial economic impacts would result in more significant industry and state reopening. Therefore, the economic and epidemiological impacts compete for any control strategy, and the proposed model tries to find a balanced strategy that

simultaneously minimizes economic and epidemiological impacts while considering the fairness in closure and reopening between industries and states.

1.3. Structure of the Dissertation

Following the introduction presented in Chapter 1, in Chapter 2 a multi-objective mixed-integer linear programming formulation is presented to minimize the pandemic policy adverse impacts by integrating and optimizing three characteristics into the formulation: epidemiologic impact of the pandemic due to open states and growing infection rate, using the SIRD model, the economic impact on the trade due to industry closure (unmet demand) using the MNFP model and the economic impact on the local businesses (lack of demand and the local businesses shrinkage). The optimization formulation is applied to the data of 11 states, the District of Columbia (including the states in New England and the mid-Atlantic,), and 19 industries. Chapter 3 provides a multi-objective mixed-integer linear programming formulation to incorporate important aspects: the epidemiologic impact using the SIRD model, the interdependencies between states and industries using the multi-regional Inoperability Input-output model, and the social fairness in the pandemic decision. The applicability of the proposed formulations are illustrated in the data of 50 states, the District of, and 19 industries in the USA. Finally, we discuss concluding remarks and prospective future work in Chapter 4.

Chapter 2: MODELING SOCIAL, ECONOMIC, AND HEALTH PERSPECTIVES FOR OPTIMAL PANDEMIC POLICY DECISION-MAKING

2.1. Introduction

Sudden Acute Respiratory Syndrome – Coronavirus-2 (SARS-Cov-2), which produces the resulting disease of COVID-19, was declared a pandemic by the World Health Organization (WHO) on January 9, 2020 (Organization, 2020). In the US, COVID-19 had its first confirmed case in Washington State on January 19, 2020 (Zimmermann et al., 2020) and as of June 20, 2021, the US has seen over 33.5 million infected cases and around 603,000 deaths. Different states started the statewide stay-at-home in late March 2020 (Chowell & Mizumoto, 2020), and critical states have considered various control strategies such as quarantine, stay-at-home, and lockdown. States, counties, and municipalities around the US have had to balance different adverse impacts of the pandemic: implement a few strategies to control the spread of the virus and potentially experience increased hospitalizations and deaths, or implement more stringent lockdown strategies and risk economic losses across several key industries. Lockdowns and business shutdowns in various states have led to business closures, increased unemployment (Blustein et al., 2020), workforce losses in critical businesses (Blustein & Guarino, 2020), and a lack of supply produced by specific industries (Chowell & Mizumoto, 2020).

As shown in Figure 2.1**,** with the growth in the active COVID cases, the number of unemployment claims increased suddenly in late March and early April, when many states and businesses started to shut down. Also, consumer behavior has changed, and the inflation

rate has grown with two months delay in late July 2020. Figure 2.1 also shows that the shutdown of the states in late March, decreased the number of active COVID cases while reopening the states in late April triggered the second wave of the COVID-19 cases.

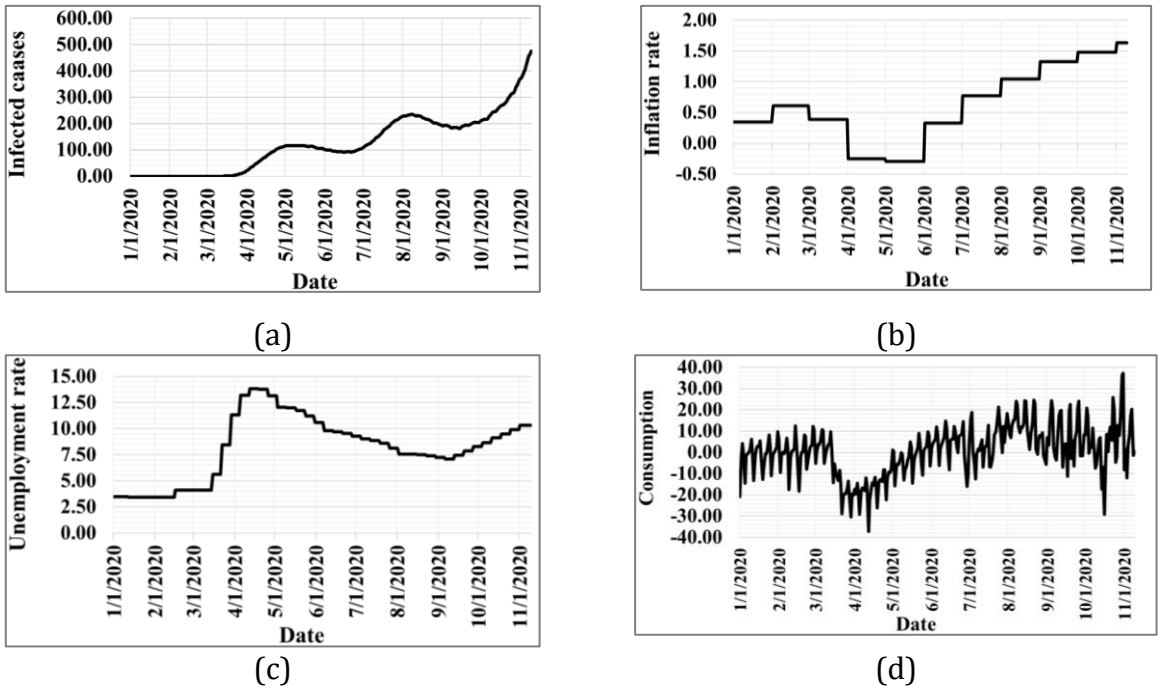

Figure 2.1. COVID-19 impacts on the economy and societal health in the US: (a) cumulative active cases per 1000 people, (b) average inflation rate, (c) average unemployment rate, and (d) average percentage change in consumption (University of Maryland, 2020).

Since the evolution of the COVID-19 pandemic, various research studies have analyzed the pandemic's social, economic, and epidemiologic impacts at international and national levels, as well as providing a wide range of policies to mitigate the crisis effect of this pandemic (Brodeur et al., 2020; Gros & Gros, 2021; Jackson et al., 2020; Nicola et al., 2020; Ocampo & Yamagishi, 2020; Principato et al., 2020; Soufi et al., 2022). Table 2. 1 summarizes selected non-clinical literature that offers a qualitative, quantitative, descriptive, and prescriptive analysis of the impact of COVID-19 on economic and societal health. According

to the literature, the epidemiological impact and the economic impact of the pandemic are tied to each other. Some research has focused on only epidemiological impact analyses through mathematical and simulation models such as different versions of the SIR (Susceptible-Infected-Recovered) model (Atkeson et al., 2020; Fernández-Villaverde & Jones, 2020; Wang et al., 2020). Other groups of research only provided the descriptive analysis of the economic impact of the pandemic by focusing on the changes in important indices such as GDP (Ehlert, 2021; McKibbin & Fernando, 2020), workforce loss (Chetty et al., 2020), and trade interruptions (Baldwin & Tomiura, 2020; Barua, 2020), among others.

According to the previous studies, lockdown and quarantine policies diminish the number of infected, hospitalized, and deceased cases. However, such policies also decrease the economic output of the closed industries, which leads to a disastrous cascading effect across other industries in the state where the strategy is enacted as well as in other states. On the other hand, opening states and industries may increase the risk of growth in infected, hospitalized, and deceased cases. Therefore, the main dilemma would be identifying an optimal control strategy and the time when it should be implemented such that the pandemic-related effects are minimized while maintaining some level of economic, health, and societal equity (Andersen et al., 2020; Ocampo & Yamagishi, 2020; Pronk & Kassler, 2020).

Table 2. 1. The literature on the analysis of COVID-19 impact on the economy and societal health.

Reference	Economic impact analysis	Epidemiologic impact analysis	Target location	Prescriptive, predictive, and quantitative model	Descriptive and qualitative model	Main considered indices
McKibbin and Fernando (2020)	*	*	Multiple	-	*	COVID cases, GDP
Baldwin and Tomiura (2020)	*	-	Multiple	-	*	Trade
Atkeson et al. (2020)	-	*	USA	SEIR	-	COVID cases
Wang et al. (2020)		*	China	SEIR	-	COVID cases
Ahmad et al. (2020)	*		Multiple		*	GDP
Abiad et al. (2020)	*	*	Multiple	-	*	COVID cases, GDP, tourism, consumption, trade
Demirguc-Kunt et al. (2020)	*	-	Multiple	-	*	COVID cases, electricity consumption, emissions
Rahman et al. (2020)	*	*	Malaysia	Data-driven clustering	-	COVID cases
(Cariappa et al., 2021)	*	-	India		*	Agricultural commodity prices, food and waste management
Chetty et al. (2020)	*	-	USA	-	*	Employment, revenue, consumption, stimulus payments, loans
Suryahadi et al. (2020)	*	-	Indonesia	-	*	Poverty
Inoue and Todo (2020)	-	*	Japan	Agent-based modeling		COVID cases
Hu (2020)	*	-	UK	-	*	Social well-being

Reference	Economic impact analysis	Epidemiologic impact analysis	Target location	Prescriptive, predictive, and quantitative model	Descriptive and qualitative model	Main considered indices
Bonet-Morón et al. (2020)	*	-	Colombia	Input-output model	-	Trade
Fernandes (2020)	-	-	Multiple	-	*	Various manufacturing and service indices
Sumner et al. (2020)	*	-	Global	-	*	Poverty
Maliszewska et al. (2020)	*	-	Global	Global general equilibrium	-	GDP, trade
(Naimoli, 2022)	-	*	Italy	HAR and ARIMA model	-	COVID cases
Barua (2020)	-	-		Standard macroeconomic AD-AS model	-	GDP, trade, exchange rates, economic growth
Dev and Sengupta (2020)	*	-	India	-	*	COVID cases, GDP, trade, electricity demand
Hevia and Neumeyer (2020)	*	-	Multiple	-	*	GDP, trade
Fernández-Villaverde and Jones (2020)	-	*	Multiple	SIRD	*	COVID cases
Choi and Shim (2021)	-	*	-	Game-theoretic epidemiologic model	-	COVID cases
(Bertsimas et al., 2021)	-	*	Global	Machine learning methods	*	COVID cases, deaths
(Aspri et al., 2021)	*	*		SEAIRD	-	COVID death cases, GDP

Reference	Economic impact analysis	Epidemiologic impact analysis	Target location	Prescriptive, predictive, and quantitative model	Descriptive and qualitative model	Main considered indices
(Chen et al., 2021)	*	*	USA	SIRD-input-output model	*	COVID death cases, Economic loss
(Lee et al., 2021)		*	USA	SIR		COVID cases

List of the abbreviations used in Table 1

GDP: Gross Domestic Product
SEIR model: Susceptible-Exposed-Infectious-Recovered model
SIRD model: Susceptible-Infected-Recovered-Deceased model
SEAIRD model: Susceptible-Exposed-Asymptomatic-Infectious-Recovered-Deceased
AD-AS model: Aggregate Demand-Aggregate Supply model
HAR model: Heterogeneous Auto-Regressive model
ARIMA model: Auto-Regressive Integrated Moving Average

Various types of research analyzed the efficacy of control strategies, specifically the closure and reopening of businesses, schools, and borders (Dickens et al., 2020; Panovska-Griffiths et al., 2020). (Zimmermann et al., 2020) quantified the economic and health risk tradeoffs of reopening industries in each state in the US. They considered income loss due to unemployment and profit loss as the economic index, which is affected by the global risk factor from the summation of four indices, including the workplace size, human interactions, inability to work from home, and industry size. The values of these four indices are impacted by the protocols designed to control the spread of the COVID pandemic. Control strategies are considered costly for firms and companies (Janiak et al., 2021; Panovska-Griffiths et al., 2020), therefore the optimal timing and scale of closure and reopening strategies are required for preventing the next wave of pandemic needs as well as minimizing the economic impact of both the pandemic and the control strategies.

The majority of the available literature has prescribed control strategies based on the descriptive analysis of the available epidemiological and economic statistics (Balla-Elliott et al., 2020; Seyedin et al., 2020; Wang et al., 2020). Few pieces of research also measured the economic and epidemiological impact of the pandemic (Chen et al., 2021). This research has several contributions to the literature. First, to the best of the authors' knowledge, no published work has proposed a mathematical model to simulate the effect of control strategies and identify the optimal closure and reopening strategies at the state and industry levels. The focus of decision-making is considered at the state and industry level because, according to the literature, the population density of states, the work environment, and the type of job can increase the chance of getting infected. The infection rate differs from one industry to another, and it depends on how people need to interact in that industry (Saidan et al., 2020; Zhou et al., 2020). Limiting close interactions in the workplace can contribute to the epidemiological impacts. Also, attending social activities, parties, and entertainment, for example, contributes to the infection rate growth (Saidan et al., 2020). State-level policies can decrease the number of such activities and the resulting chance of the spread of the virus. Second, this paper proposes a novel multi-objective mixed-integer linear programming (MOMILP) model that integrates a modified version of the susceptible-infected-recovered-deceased (SIRD) epidemiological model, a modified maximum network flow problem, and a model to measure the economic impact on local businesses. The three models are connected through state-level and industry-level decisions. The optimization-based model provides prescriptive solutions which can control specified aspects of the pandemic impact. Also, the integration allows decision-makers to emulate and analyze the dynamic competition between the economic and epidemiological aspects of the controlling policy. Third, the

proposed model results in a temporal decision and allows decision-makers to identify the optimum pandemic policy for a desired planning time horizon.

2.2. Problem Formulation

The proposed MOMILP evaluates and minimizes the effects of the dynamic closure and reopening strategies during the pandemic crisis, providing the optimal control strategies to decision-makers for (i) each industry, (ii) each state, and (iii) each period. With such an optimization framework, we look to address different decision-making perspectives: state-level decisions, national-level decisions, industry-level decisions, and how any of these trade-offs with each other.

The proposed model considers three objectives including (i) the epidemiological impact of the pandemic in terms of the percentage of the infected population, (ii) the economic impact of the pandemic on the local businesses in terms of the percentage of decrease in the business's employees, and (iii) the economic impact of the pandemic on the amount of commodity traded between industries in terms of the unmet demand percentage in industries and states. The epidemiological and economic impacts on businesses and industries are the very first tangible impact of the pandemic (Alsharef et al., 2021; Fairlie & Fossen, 2021). A non-comprehensive state and industry level policy for controlling pandemics would propagate the epidemiological and economic impact of a pandemic to the other aspects of socio-economic systems, causing other negative impacts such as social in-equity, unequal poverty changes, unbalanced vaccination distribution, adverse change in education systems, among others (Martin et al., 2020; Mishra et al., 2020). Each of these impacts can be considered an individual objective when one tries to optimize the pandemic

policy. However, controlling the early impacts can help with minimizing the later impacts. Therefore, in this study, we are only considering the two impacts caused by state and industry closure and reopening, as the building blocks for early analysis and a decision tool that provide short-term emergency actions.

Figure 2. 2 shows the dynamics of the impacts created by the state- and industry-level decisions on the economic and epidemiological aspects. The closure of states and industries would lead to adverse economic consequences while decreasing the adverse epidemiological impacts. The economic impact is measured here as a two-fold effect, including (i) the economic impact on trade and (ii) the economic impact on local businesses. The economic impact of industry closure is measured by the met/unmet demand of each state from the commodity of each industry at each time. This measure represents the inability of industries to satisfy the inter-industry and consumer demand at the state level, caused by policy-driven closure or by workforce productivity losses due to the pandemic. In this paper, we refer to this effect as the *economic impact on trade*. Also, the state closure would decrease the demand for certain service businesses such as entertainment, accommodation and food services, hotels, transportation, and education, among others. According to (Fairlie & Fossen, 2021), the pandemic and related social distancing, quarantine, and state closure policies have hurt different industries by shrinking the number of active businesses due to the shift in the demand for those industries. The drop in the number of active businesses causes a negative economic impact mainly by a higher unemployment rate. We measure the economic impact of the state closure policies by the percentage of shrinkage in these local businesses in terms of the percentage of employees whose jobs were lost. In this paper, we refer to this effect as the *economic impact on local businesses*. On the other hand, the increase in the

negative epidemiological impact would result in workforce losses, leading to the inability of industries to have optimal productivity and may result in business closures. Since there is no reliable data available for such impact, the proposed model does not consider the later effect of the pandemic in the analysis.

The epidemiological impact in terms of the percentage of the infected population is measured based on the proposed modified dynamic SIRD model. The modified dynamic SIRD model represents the changes in four main population categories: infectious, susceptible, recovered/immune, and deceased individuals. It is assumed that the pandemic growth rate differs by state and industry, as the population density and the employment density vary by state and industry. More adverse epidemiological impacts result in more industry and state closures, while more substantial economic impacts would result in more significant industry and state reopening. Therefore, the economic and epidemiological impacts compete for any control strategy, and the proposed model tries to find a balanced strategy that simultaneously minimizes economic and epidemiological impacts.

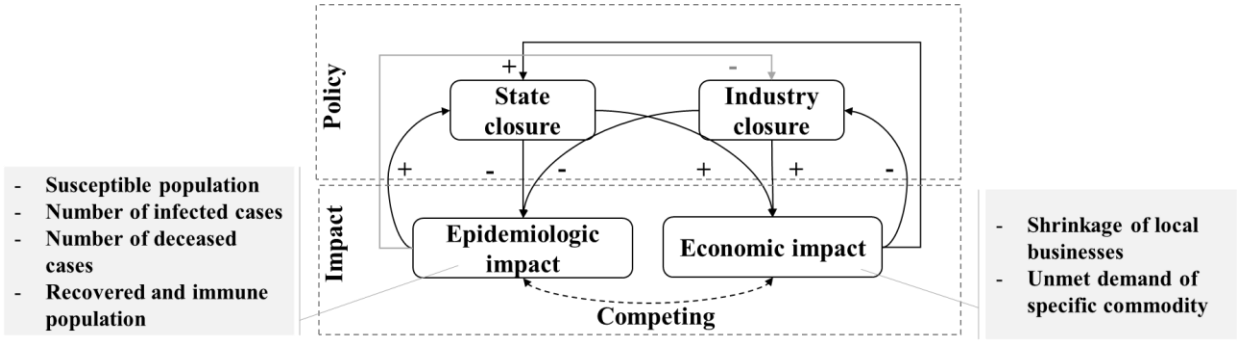

Figure 2. 2. The dynamics of the relationship between pandemic policy and the economic and epidemiological impacts.

To measure the economic impact on trade due to an industry closure, we are using the multi-commodity maximum network problem. Also, the economic impact on local businesses is caused by a state closure and is measured by the number of employees that lose their job in local businesses. The epidemiological impact of industry and state reopening strategies is measured with the modified SIRD model. To depict the economic and epidemiological impact of state and industry closure and reopening, the three models are combined with two decision variables: state status and industry status. In the following, we explain the concepts of the MNFP and the SIRD models that are used later in the proposed mixed-integer programming model.

2.2.1. Maximum Network Flow Problem

Let $G = (N, L)$ be an undirected connected network, where N is the set of states represented by nodes, and L is the set of trade links between each pair of states. K is a set of industries producing specific commodities divided into two subsets. The first subset is the set of industries producing commodities traded between two states ($K_1 \subseteq K$ and K_1 is the set of industries producing tradable commodities). The second subset is the set of industries producing commodities consumed only inside the state ($K_2 \subseteq K$ and K_2 is the set of industries producing non-tradable commodities, including the local businesses such as restaurants and theaters, among others). Each state can be considered either a supply, demand, or transshipment node in the MNFP model, for each commodity of industry $k \in K$ and at each time. Therefore, one dummy supply node is capacitated with the state production level for each commodity, and one dummy demand node is defined for every state. In the MNFP, N denotes the set of nodes that consist of $N_=$ as the actual states and the

transshipment nodes, N_+ as the set of dummy supply nodes, and N_- as the set of dummy demand nodes. Each link $(i, j) \in L$ has a specified capacity u_{ij} for transferring the flow of materials of any kind, shown in constraint (2.2), in which x_{ij}^k denotes the flow of commodity of industry k between state i and j. The multi-commodity maximum network flow problem tries to maximize the flow between two nodes (Iri, 1971) such that it satisfies the demand of each node from each commodity, considering the constraints of the link capacity, u_{ij}, supply capacities, c_i^k, and demand d_i^k, shown in constraints (2.2)-(2.4). This formulation can also be equivalent to an optimization problem that minimizes the total unmet demand in the network stemming from the non-optimum flow between every two nodes, as shown in the objective function in Eq. (2. *1)*. in Eq. (2. *1)* measures the total unmet demand over all commodities and all states by quantifying the difference between the inflow of each commodity into each state at each time ($\sum_{j \in N} x_{jit}^k$) and the state's demand for that commodity (d_i^k), then summing over all calculated unmet demands over states, commodities, and the time horizon. In addition, in our proposed MNFP problem, the supply capacity, c_i^k, will be forced to be zero for closed industries. Constraint (2.5) shows the flow balance in transshipment nodes. Constraint (2.6) ensures that in a balanced economic system, the total supply of each commodity of industry $k \in K$ should be equal to the total demand for that commodity. We add one more constraint to the MNFP model to ensure that the trade of non-tradable commodities, $k \in K_2$, between states is not allowable, as shown by constraint (2.7).

$$\min \quad \sum_{i\in N}\sum_{k\in K}\left(d_i^k - \sum_{j\in N} x_{ji}^k \right) \tag{2.1}$$

$$\sum_{k\in K} x_{ijt}^k \le u_{ij} \qquad \forall\,(i,j)\in L\,,\ t=1,\dots,T \tag{2.2}$$

$$\sum_{j:(i,j)\in L} x_{ijt}^k \le c_i^k \qquad \forall i\in N_+,\ t=1,\dots,T, \forall\, k\in K \tag{2.3}$$

$$\sum_{j:(j,i)\in L} x_{jit}^k \le d_i^k \qquad \forall i\in N_-,\ \ t=1,\dots,T, \forall\, k\in K \tag{2.4}$$

$$\sum_{j:(i,j)\in L} x_{ijt}^k - \sum_{j:(i,j)\in L} x_{jit}^k = 0 \qquad \forall i\in N,\ t=1,\dots,T, \forall\, k\in K \tag{2.5}$$

$$\sum_{\substack{k\in K \\ \forall\ i\in N_+}} \sum_{j:(i,j)\in L} x_{ijt}^k - \sum_{\substack{k\in K \\ \forall\ i\in N_-}} \sum_{j:(j,i)\in L} x_{jit}^k = 0 \qquad t=1,\dots,T, \forall\, k\in K \tag{2.6}$$

$$\sum_{j\neq i:(i,j)\in L} x_{ijt}^k = 0 \qquad \forall i,j\in N_=,\ t=1,\dots,T, \forall\, k\in K_2 \tag{2.7}$$

2.2.2. Modified SIRD Model

The susceptible-infected-recovered-deceased (SIRD) model is a well-known mathematical representation of the dynamics of an epidemic or a pandemic (Zhu et al., 2019). The SIRD model is governed by ordinary differential equations or fractional differential derivatives (Kermack & McKendrick, 1927). According to this model, a susceptible person is a person prone to infection when coming in contact with an infected person. The infected person can either recover from the infection or die after the infection. It is assumed that there is no latent time between exposure to the disease and getting infected. The SIRD model is governed by ordinary differential equations or fractional differential derivatives (Kermack & McKendrick, 1927). It formulates the relation between the numbers of susceptible cases $S(t)$, infected cases $I(t)$, recovered cases $R(t)$, and deceased cases $D(t)$ at each time and in a certain population. The differential equations of the SIRD model, shown in Eqs. (2.8)-(2.11),

describe the changes in each of the four categories of cases based on the infection rate, α, recovery rate, ρ, and mortality rate, γ, while η is the sum of the susceptible cases $S(t)$, infected cases $I(t)$ and recovered cases $R(t)$.

$$\frac{dS(t)}{dt} = -\frac{\alpha}{\eta} I(t)S(t) \tag{2.8}$$

$$\frac{dI(t)}{dt} = -\frac{\alpha}{\eta} I(t)S(t) - \rho I(t) - \gamma I(t) \tag{2.9}$$

$$\frac{dR(t)}{dt} = \rho I(t) \tag{2.10}$$

$$\frac{dD(t)}{dt} = \gamma I(t) \tag{2.11}$$

The SIRD model is a highly nonlinear and complex model that simulates the pandemic dynamics considering the initial infectious and the infection, recovery, and mortality rate. To adapt the SIRD model to the COVID pandemic specifications in our proposed MOMILP, we add the following assumptions to the SIRD model.

1. The susceptible population gets infected with a specific infection rate of α in state i.
2. The infected population is recovered with a recovery rate ρ and after a specific time of t_R since infection, or they die at a specific time t_D periods after their infection, with a death rate of γ.
3. The recovered population maintains immunity status for a specific immunity time of t_I before they go back to the susceptible population.

Figure 2. 3 shows the schematic of the relationship between susceptible $S(t)$, infectious $I(t)$, recovered $R(t)$, and deceased $D(t)$ cases considering the required modifications in the time concepts. By incorporating the recovery time and the immunity time, the infected

population who will recover from the disease would enter the susceptible population after $(t_R + t_I)$.

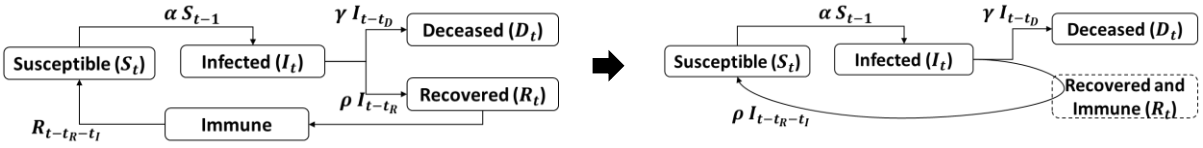

Figure 2. 3. The conceptual schema for the relationship between susceptible S(t), infectious P(t), recovered R(t), and deceased D(t) cases in the modified dynamic SIRD model.

2.2.3. Proposed MOMILP Model

The proposed model combines the modified MNFP and the modified SIRD model to optimize the timing of the implementation of control strategies. Eqs. (2.12)-) show the proposed MOMILP model in the form of a mixed-integer program. The definition of sets and the notation of the parameters and decision variables are shown in Table 2. 2, Table 2. 3, and Table 2. 4, respectively

Table 2. 2. Model indices and sets.

Set	Definition
N	Set of all states indexed by $i \in I$ and $j \in I$ (e.g., state 2)
N_+	Set of all dummy supply nodes indexed by $i \in N$
N_-	Set of all dummy demand nodes indexed by $i \in N$
K	Set of all industries indexed by $k \in K$, such that $K_1, K_2 \subseteq K$ and $k \in K_1$ indexes the industry producing tradable commodities and $k \in K_2$ indexes the industry producing non-tradable commodities.
L	Set of all links connecting two states indexed by $(i, j) \in L$

Table 2. 3. Model parameters.

Parameters	Definition
$\boldsymbol{c_i^k}$	The supply capacity of the state i for the commodity of industry k
$\boldsymbol{d_i^k}$	The demand of state i from the commodity of industry k
$\boldsymbol{u_{ij}}$	The capacity of the link $(i,j) \in L$
$\boldsymbol{\alpha_i}$	The infection rate in state i
$\boldsymbol{\beta^k}$	The infection rate in industry k
$\boldsymbol{\rho}$	Recovery rate in the country
$\boldsymbol{\gamma_i}$	COVID death rate in state i
$\boldsymbol{a_i}$	The initial susceptible population in state i (equal to the initial population of state i)
$\boldsymbol{b_i}$	The initial number of patients in state i
$\boldsymbol{g_i}$	The initial status of the state i
$\boldsymbol{f_i^k}$	The initial status of the state i for industry k
$\boldsymbol{e_i^k}$	The initial number of employees in state i for industry k
$\boldsymbol{q^k}$	The shrinkage of industry $k \in K_2$ (local businesses) in terms of the percentage of employees whose jobs were lost due to the state closure.
$\boldsymbol{t_R}$	The average recovery period ($\sim$ 20 days)
$\boldsymbol{t_I}$	The average immunity period ($\sim$ 90 days)
$\boldsymbol{t_D}$	The average death period ($\sim$ 10 days)
$\boldsymbol{m}$	Large number
$\boldsymbol{t}$	The index of time ranging from 1 to time horizon T

Table 2. 4. Model decision variable.

Variable	Definition
x_{ijt}^k	The flow of commodity of industry k on link $(i,j) \in L$ at time $t = 1, \dots, T$, continuous
v_{it}^k	The met demand of commodity of industry k in the state i at time $t = 1, \dots, T$, continuous
p_{it}	Number of patients in state i at time $t = 1, \dots, T$, integer
w_{it}	Number of new patients in state i at time $t = 1, \dots, T$, integer
s_{it}	Number of total susceptible people in state i at time $t = 1, \dots, T$, integer
r_{it}	Number of susceptible people to infection in state i at time $t = 1, \dots, T$, integer
o_{it}^k	Number of total susceptible employees in state i and industry k at time $t = 1, \dots, T$, integer
n_{it}^k	Number of total susceptible employees to infection in state i and industry k at time $t = 1, \dots, T$, integer
y_{it}^k	Equal to 1 if industry k in state i is open at time $t = 1, \dots, T$, binary
z_{it}	Equal to 1 if state i is open at time $t = 1, \dots, T$, binary

The proposed MOMILP model contains three distinct objective functions shown in Eqs. (2.12)-(2.14), including: (i) the epidemiological impact in terms of the percentage of the infected population across the states (F1), (ii) the economic impact on local businesses (LB) in terms of the percentage of total unemployment due to the state closure across industries and states (F2), and (iii) the economic impact on trade in terms of the percentage of total unmet demand across industries and states (F3). As shown in Figure 2. 2, the epidemiological impact (F1) and the economic impacts (F2 and F3) compete such that any strategy that decreases the epidemiological impact by state and industries closure would result in an increase in economic impact due to a higher percentage of unmet demand and shrinkage of local businesses, and vice versa. Therefore, the MOMILP model balances all three objectives simultaneously: Eqs. (2.12), (2.13), and (2.14).

The epidemiologic impact measures the number of infected people who are infected either in their social life or during their work time. Depending on the status of the states and industries, the number of new patients can be calculated using Eq. (2.45) and being used as a constraint in the MOMILP model to update the number of infected people. However, this equation makes the MOMILP model nonlinear optimization programming. Therefore, new decision variables $r_{i(t)}$ and $n^k_{i(t)}$ are defined to linearize Eq. (2.45) and turn it into multiple linear equations shown in constraints (2.24)-(2.31).

$$\text{F1: min} \quad \sum_{t=1}^{T} \sum_{i \in N} \left(\frac{p_{it}}{a_i} \right) \tag{2.12}$$

$$\text{F2: min} \quad \sum_{t=1}^{T} \sum_{i \in N} \left(\frac{\sum_{k \in K} q^k e_i^k \, (1 - z_{it})}{\sum_{k \in K} e_i^k} \right) \tag{2.13}$$

F3: min $\sum_{t=1}^{T}\sum_{i\in N}\sum_{k\in K}\left(1-\frac{v_{it}^{k}}{d_{i}^{k}}\right)$ (2.14)

s. t.

$\sum_{k\in K} x_{jit}^{k} \le u_{ij}$ $\forall(i,j)\in L\ ,\ t=1,\dots,T$ (2.15)

$\sum_{j:(i,\,j)\in L} x_{ijt}^{k} = c_{i}^{k}\, y_{it}^{k}$ $\forall i\in N_{+}, \forall\ k\in K,\ t=1,\dots,T$ (2.16)

$\sum_{j:(j,i)\in L} x_{jit}^{k} = v_{it}^{k}$ $\forall i\in N_{-}, \forall\ k\in K,\ t=1,\dots,T$ (2.17)

$v_{it}^{k} \le d_{i}^{k}$ $\forall i\in N_{-}, \forall\ k\in K,\ t=1,\dots,T$ (2.18)

$\sum_{j:(i,\,j)\in L} x_{ijt}^{k} - \sum_{j:(i,\,j)\in L} x_{jit}^{k} = 0$ $\forall i\in N,$ $\forall\ k\in K,\ t=1,\dots,T$ (2.19)

$\sum_{j\neq i:(i,\,j)\in L} x_{ijt}^{k} = 0$ $\forall i\in N_{=}, \forall\ k\in K_{2},\ t=1,\dots,T$ (2.20)

$\sum_{i\in N_{+}}\sum_{k\in K}\sum_{\substack{j:(i,\,j)\in L\\ i\in N_{+}}} x_{ijt}^{k} - \sum_{i\in N_{-}}\sum_{k\in K}\sum_{\substack{j:(j,i)\in L\\ i\in N_{-}}} x_{jit}^{k} = 0$ $t=1,\dots,T$ (2.21)

$p_{it} = p_{i(t-1)} + w_{i(t-1)} - \gamma_{i} w_{i(t-t_{D})} - (1-\gamma_{i}) w_{i(t-t_{R})}$ $\forall i\in N_{+},\ t=1,\dots,T$ (2.22)

$w_{it} = \alpha_{i}\left(r_{it} - \sum_{k\in K} n_{it}^{k}\right) + (1 - (1-\alpha_{i})\left(1-\beta_{i}^{k}\right)) \sum_{k\in K} n_{it}^{k}$ $\forall i\in N_{+},\ t=1,\dots,T$ (2.23)

$s_{it} = s_{i(t-1)} + (1-\gamma_{i}) w_{i(t-t_{R}-t_{I})} - w_{i(t-1)}$ $\forall i\in N_{+},\ t=1,\dots,T$ (2.24)

$s_{it} \le r_{it} + m(1-z_{it})$ $\forall i\in N_{+},\ t=1,\dots,T$ (2.25)

$$s_{it} \geq r_{it} \qquad \forall i \in N_+,\ t = 1, \dots, T \qquad (2.26)$$

$$r_{it} \leq m\, z_{it} \qquad \forall i \in N_+,\ t = 1, \dots, T \qquad (2.27)$$

$$o_{it}^k = o_{i(t-1)}^k - (1-\gamma_i)\,\beta_i^k n_{i(t-t_R-t_I)}^k - \beta_i^k n_{i(t-(t_R+t_I))}^k \qquad \forall i \in N_+, \forall\, k \in K,\ t = 1,\ \dots, T \qquad (2.28)$$

$$o_{it}^k \leq n_{it}^k + m(1 - y_{it}^k) \qquad \forall\, i \in N_+, \forall\, k \in K,\ t = 1, \dots, T \qquad (2.29)$$

$$o_{it}^k \geq n_{it}^k \qquad \forall\, i \in N_+, \forall\, k \in K,\ t = 1, \dots, T \qquad (2.30)$$

$$n_{it}^k \leq m\, y_{it}^k \qquad \forall\, i \in N_+, \forall\, k \in K,\ t = 1, \dots, T \qquad (2.31)$$

$$p_{it} \leq a_i \qquad \forall i \in N_+,\ t = 1,\ \dots, T \qquad (2.32)$$

$$s_{it} \leq a_i \qquad \forall i \in N_+,\ t = 1,\ \dots, T \qquad (2.33)$$

$$o_{it}^k \leq e_i^k \qquad \forall\, i \in N_+, \forall\, k \in K,\ t = 1, \dots, T \qquad (2.34)$$

$$s_{it} = r_{it} = a_i \qquad \forall i \in N_+,\ t = 0 \qquad (2.35)$$

$$o_{it}^k = n_{it}^k = e_i^k \qquad \forall\, i \in N_+, \forall\, k \in K,\ t = 0 \qquad (2.36)$$

$$p_{it} = b_i \qquad \forall i \in N_+,\ t = 0 \qquad (2.37)$$

$$z_{it} = g_i \qquad \forall i \in N_+,\ t = 0 \qquad (2.38)$$

$$y_{it}^k = f_i^k \qquad \forall\, i \in N_+, \forall\, k \in K,\ t = 0 \qquad (2.39)$$

$$y_{it}^k \in \{0,1\} \qquad \forall i \in N_+, \forall\, k \in K, t = 1, \dots, T \qquad (2.40)$$

$$z_{it} \in \{0,1\} \qquad \forall i \in N_+, t = 1, \dots, T \qquad (2.41)$$

$$p_{it},, s_{it}, r_{it} \geq 0 \qquad \forall i \in N_+, t = 1, \dots, T \qquad (2.42)$$

$$o_{it}^k, n_{it}^k, v_{it}^k \geq 0 \qquad \forall i \in N_+, \forall\, k \in K, t = 1, \dots, T \qquad (2.43)$$

$$x_{ijt}^k \geq 0 \qquad \forall (i,j) \in L\,, \forall\, k \in K,\ t = 1, \dots, T \qquad (2.44)$$

The modified MNFP is represented in constraints (2.15)-(2.21). Constraints (2.15)-(2.18) generate the bounds on supply, demand, and trade between states. When the objective

function F3 minimizes the unmet demand in each state at each time, the flow of commodities between states is maximized to its upper bound level. Constraint (2.15) limits the amount of trade of commodity of industry k between states i and j up to the capacity of the transportation channel between two states. The upper bound for the trade capacity, u_{ij}, is calculated from the amount of actual trade between two states. Constraint (2.16) balances the supply of industry k in each state i, if and only if the industry k is open in that state. The binary variable y_{it}^{k} forces the constraint (2.16) to consider the supply capacity of industry k in state i, if that industry is open at time t. If industry k in state i does not exist or is not open, then the state i demands or transships the commodity of industry k. In this case, the net input of commodity of industry k onto state i cannot surpass the actual demand of state i for the commodity of industry k. These conditions are shown in constraints (2.17) and (2.18). Constraint (2.19) ensures the flow balance for all nodes, and constraint (2.20) ensures that for non-tradable industries, the flow of commodity of industry k between states is zero. Constraint (2.21) guarantees that the total produced commodity of industry k in the entire network of states is equal to the total consumed commodity of industry k.

Constraints (2.23)-(2.34) generate the bounds for the modified SIRD model and the linearization process of this model. Constraint (2.22) updates the number of patients at each time based on the number of patients in the previous period, the newly infected people (W_{it}), the number of recovered cases at the time $t - t_R$ and the number of deceased cases at the time $t - t_D$. Constraint (2.23) updates the number of new infectious (patients) based on the status of industries and states. It is assumed that every susceptible person may become infected during their work life or social life (except during work hours). Constraint (2.23) is formulated to avoid double counting an employee's chance of infection during their work life

and social life. In constraint (2.23), if the states are open ($z_{it} = 1$) and the industries are open ($y_{it}^k = 1$), then there will be some new infections in each state equal to $\alpha_i s_{i(t-1)} z_{it}$, and there will be some new infections in each industry equal to $\sum_k \beta_i^k o_{i(t-1)}^k y_{it}^k$. With this logic, the number of new patients could be calculated using Eq.(2.45).

$$W_{it} = \alpha_i \left(\alpha_i s_{i(t-1)} z_{it} - \sum_{k \in K} \sum_{k \in K} \beta_i^k o_{i(t-1)}^k y_{it}^k \right) + (1 - (1 - \alpha_i)(1 - \beta_i^k)) \sum_{k \in K} \beta_i^k o_{i(t-1)}^k y_{it}^k \quad \forall i \in N,\ t = 1, \dots, T \tag{2.45}$$

However, the above formulation is nonlinear. To linearize this constraint, we introduce constraints (2.24)-(2.31) and new decision variables r_{it} and n_{it}^k. We replace decision variables s_{it} and o_{it}^k in constraint (2.45) with new decision variables $r_{i(t)}$ and $n_{i(t)}^k$ and turn this constraint into the constraint (2.23). Constraints (2.24)-(2.27) update the number of susceptible populations in each state at each time, considering the status of that state. If the state i is open at time t, then $r_{i(t-1)} = s_{i(t-1)}$ will be used in constraint (2.24)-(2.27), otherwise $r_{i(t-1)} = 0$ and there are no new infections in state i. Constraints (2.28)-(2.31) update the number of available workforces in industry k in each state at each time considering the status of that industry. If industry k in state i is open at time t, then $n_{i(t-1)}^k = o_{i(t-1)}^k$ being used in constraints)-(2.31), otherwise $n_{i(t-1)}^k = 0$ and there will be no new infections in industry k in state i.

Constraints (2.32)-(2.34) limit the infected and susceptible populations in each state to its total population and the infected workforce of industry k in state i to its total number of

employees. Constraints (2.35)-(2.41) define the initial value for each decision variable at time $t = 0$, and constraints)-(2.44) denote the nature of decision variables.

2.3. Illustrative Example

The proposed model is illustrated with several sources of data describing industry productivity, as well as state and COVID pandemic characteristics.

2.3.1. Data

The data used in this research are divided into two categories as follows.

1. COVID-19 data: These data include the COVID-19-related rates, including the infection, recovery, and death rate at the state level in the United States. These data are gathered from the COVID-19 Impact Analysis Platform compiled by the University of Maryland(University of Maryland, 2020). The average proportion of the total recovery to the total active cases all around the US is equal to 0.6. Data related to the recovery time, death time, and immunity time frame are gathered from the literature and reports from the Centers for Disease Control and Prevention (CDC)[1]. The infection rate in each industry is derived from the Washington state department of health report(Department of Health, 2020). These data show the COVID infection rate in different industries in Washington state, and we have used the same rate for similar industries in all other states.

1 https://www.cdc.gov

2. Economic data: The required data for the MNFP model is derived from the Commodity Flow Survey published by the Bureau of Transportation Statistics(Bureau of Transportation Statistics, 2020). These data show the yearly trade from each commodity/industry and between each pair of states in 2017. It is assumed that the links between two states can handle the flow of commodities up to their yearly trade. Each state's supply and demand capacity for each industry is also calculated from the same survey such that Eqs. (2.46) and (2.47) hold, where f_{ij}^{k} is the actual flow of commodity produced by industry k (\$ 1/1000), traded between from state i to state j.

$$c_i^k = \sum_{j:(i,\, j)\in L} f_{ij}^k \qquad \forall i \in N, \forall k \in K \tag{2.46}$$

$$d_i^k = \sum_{j:(i,\, j)\in L} f_{ji}^k \qquad \forall i \in N, \forall k \in K \tag{2.47}$$

Note that to consider the supply of each state from the commodity of the industries which exist in that state, we need to consider all nodes as supply nodes (using dummy supply nodes). Therefore, we do not calculate pure supply and demand nodes by subtracting the output flow from the input flow of each commodity in each state; alternatively, we use the results of Eqs. (2.46) and (2.47) calculate the actual supply and demand capacity. Employment statistics at the state and industry levels are derived from the US Bureau of Labor Statistics(Bureau of Labor Statistics, 2022).

In this study, the data of 11 states, the District of Columbia (including the states in New England and the mid-Atlantic,), and 19 industries are considered. Table 2. 5 shows the definition of the industries and their North American Industry Classification System (NAICS)

code, along with their industry-specific rate of COVID-19 infection and the rate of local business shrinkage due to state closure.

Table 2. 5. The definition of the industries considered in this study.

NAICS code	Industry definition	Infection rate (%)	Business shrinkage (%)
Tradable industries (K_1)			
21	Mining, Quarrying, and Oil and Gas Extraction	1	-
31-33	Manufacturing	9	-
42	Wholesaler's trade	3	-
45	Retail trade	10	-
49	Transportation and Warehousing	5	-
51	Information	1	-
55	Management of Companies and Enterprises	2	-
Non-tradable industries (K_2 or local businesses)			
11	Local Agriculture, Forestry, Fishing, and Hunting	9	-0.875
23	Local Construction	8	3.375
48	Local Transportation and Warehousing	5	2.75
52	Finance and Insurance	2	1.5
53	Real Estate and Rental and Leasing	2	2.125
56	Administrative and Support, and Waste Management and Remediation Services	4	2.125
54	The Professional, Scientific, and Technical Services	4	2.25
61	Educational Services	4	4.875
62	Health Care and Social Assistance	24	2
71	Arts, Entertainment, and Recreation	1	4.375
72	Accommodation and Food Services	5	2.75
81	Other Services (except Public Administration)	3	6.5

Table 2. 5 shows the infection and death rate at the state level and the size of each industry in each state based on the number of employees of that industry. It is assumed that industries only use the freight network within the US to trade

commodities. Therefore, each state is connected to its closest neighboring states, and 352 arcs are considered in the modified MNFP model.

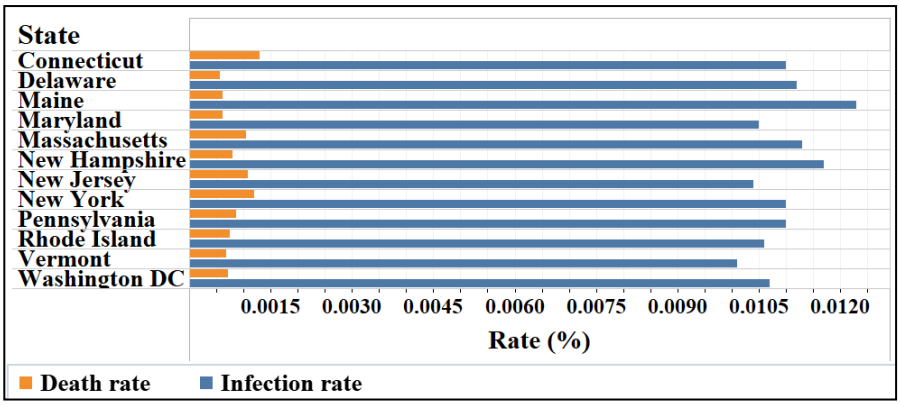

(a)

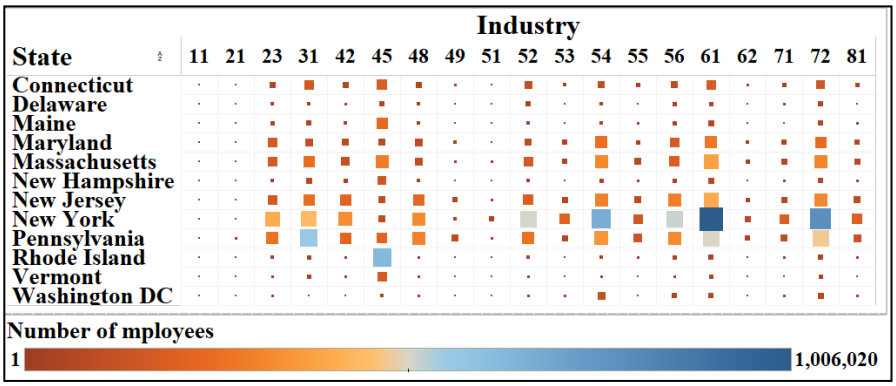

(b)

Figure 2. 4. The input variables at the state and industry levels. (a) The COVID-19 infection and death rate at the state level. (b) The size of each industry in each state is based on the number of employees.

Figure 2. 5 shows the value of traded commodities of 19 industries from each state to the other states. According to these data, Pennsylvania and New York are the states with the highest export and import of commodities. Also, the *Manufacturing* industry has the highest value of products being traded between states, followed by the *Wholesale trade* and *Warehouse and storage*. Therefore, the closure of these industries is expected to cause a high rate of unmet demand systems.

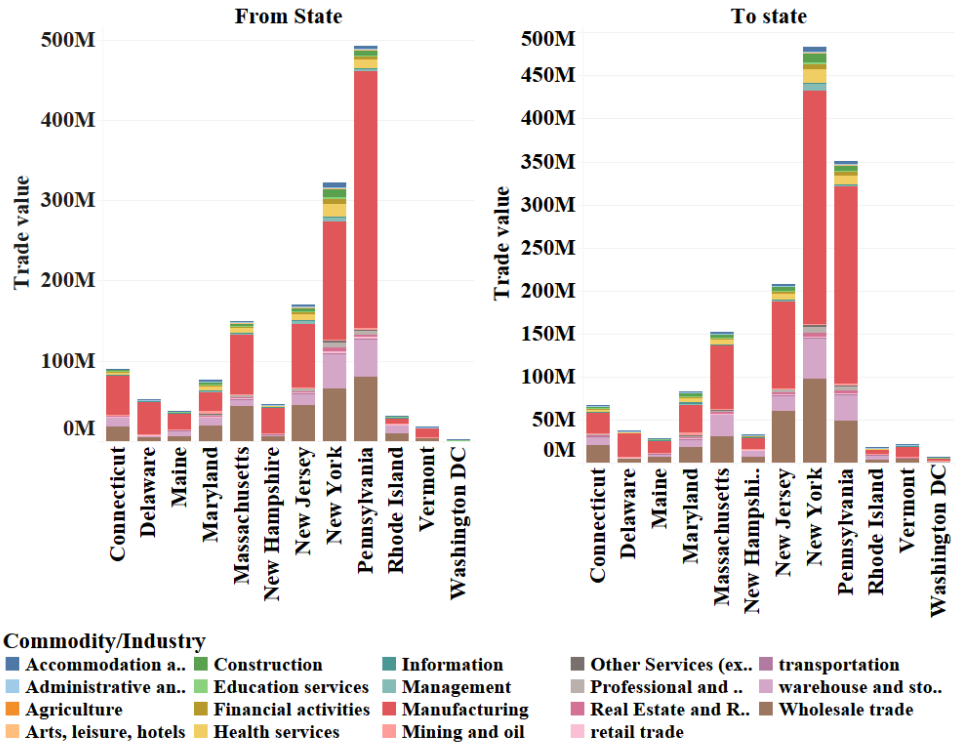

Figure 2. 5. The trade value of commodities of 19 industries from and to the 11 states.

According to Kyrychko et al. (2020), the mean value of time to recovery, t_R, is 15.3 days, and the mean value of the time to death, t_D, is nine days. Therefore, the time interval in our analysis is equivalent to 10 days. Therefore, we assume that $t_R = 2$ (equivalent to 20 days) and $t_D = 1$ (equivalent to 10 days). According to the CDC[2] (Center for Disease Control and Prevention), evidence suggests that reinfection is uncommon 90 days after the initial infection. Therefore, we consider the immunity time $t_V = 9$ in the model. At the initial time $t = 0$, all industries, and states are considered open.

2 https://www.cdc.gov/

2.3.2. Solution Approach

There are three solution approaches for solving a multi-objective optimization problem (Hwang & Masud, 2012), including (i) *a-priori* methods (e.g., weighted-sum method); (ii) interactive methods, and (iii) the generation (or *a-posteriori*) methods (e.g., ε-constraint method). Recall that in the proposed objective function in Eq. (2.12)-(2.14), there are three different objectives with different ranges and scales. Therefore, in this study, we utilize the augmented ε-constraint method proposed by (Mavrotas & Florios, 2013) to solve the proposed multi-objective MOMILP model. The augmented ε-constraint method (AUGMECON) is an efficient version of the ε-constraint method, which accelerates the process of generating Pareto-optimal solutions by avoiding redundant iterations. By individually considering each objective as the primary objective and the other two objectives as secondary objectives, we formulate, solve, and compare the results of three different versions of AUGMECON models. For example, the AUGMECON formulation of considering epidemiological impact (F1) as the primary objective function and considering the economic impact on local businesses (F2) and economic impact on trade (F3) as two secondary objectives will be represented as follows, in which s_l is the non-negative slack variable showing the amount of deviation of the secondary objective function l from its optimum value. The RHS value of constraint (2.49) is $e_l = ub_l - (L_l \times r_l)/g_l$ where ub_l is the upper bound of the secondary objective function l and L_l is the iteration counter of the grid points in the solution grid of g_l. Term r_l is the range of the secondary objective function l in the payoff matrix (upper bound, ub_l, to lower bound, lb_l), respectively. X is the feasibility area for the original MOMILP. A similar structure is built for the cases in which the economic impact on local businesses (F2) or the economic impact on trade (F3) is considered the primary objective.

$$\min \sum_{t=1}^{T}\sum_{i\in N}\sum_{k\in K}\left(1-\frac{v_{it}^{k}}{d_{i}^{k}}\right)- eps\left(\frac{s_1}{r_1}+\frac{s_2}{r_2}\right) \tag{2.48}$$

s.t.

$$\sum_{t=1}^{T}\sum_{i\in N}\left(\frac{p_{it}}{a_i}\right)+ s_1 = e_1 \tag{2.49}$$

$$\sum_{t=1}^{T}\sum_{i\in N}\left(\frac{\sum_{k\in K} q^k e_i^k\,(1-z_{it})}{\sum_{k\in K} e_i^k}\right)+ s_2 = e_2 \tag{2.50}$$

$$y_{it}^{k}, z_{it}, p_{it},, s_{it}, r_{it}, o_{it}^{k}, n_{it}^{k}, v_{it}^{k},\ x_{ijt}^{k} \in X \tag{2.51}$$

Practically, the AUGMECON algorithm (Mavrotas & Florios, 2013)is as follows: (i) Generate the payoff matrix using conventional or lexicographic optimization (the table with the results from the optimization of each function individually). (ii) Calculate the range of values of each objective function l, denoted as r_l. (iii) Divide each r_l into equal intervals h_l using the intermediate equidistant grid point such that we have the total $(h_l + 1)$ grid points that are used to vary the RHS values of e_l parametrically. The number of grid points will determine the density of the efficient set of the solution as well as the computation time. (iv) Solve the model by choosing each point in the grid and determining the value of e_l. If the model becomes infeasible for a specific point of the grid, the model avoids running for the lower values of e_l in that specific direction. More detail on the AUGMECON method can be found in (Mavrotas & Florios, 2013).

All the implementations in this study are performed on a 64-bit desktop system with 12.0 GB RAM and the Core-i7-6500U CPU@2.5GHz. The proposed framework is modeled and

solved by Gurobi in Python, and for the selected time horizon T, the average run time is reported in the next section.

2.4. Results

In this study, we consider six different scenarios, as shown in Table 2. 6, in which we analyze the quality of calculated solutions by solving the model for different objective functions. The proposed model considers only one objective in the first three scenarios and is solved as a single objective MILP. In the latter three scenarios, the proposed model will be solved as a multi-objective MILP using the AUGMECON method by considering one of the objectives as the primary objective function one at a time.

Table 2. 6. The definition of the scenarios

Scenario	Objective function	Objective
1	Min F1	Minimizing the epidemiological impact (F1)
2	Min F2	Minimizing the economic impact on local businesses (F2)
3	Min F3	Minimizing the economic impact on trade (F3)
4	Min MOMILP	Minimizing the MOMILP using the AUGMECON method

The MOMILP model will result in a set of Pareto-optimal solutions instead of a single optimal solution. To generate the Pareto optimum solutions, we consider 6×6 grid points and solve scenarios 4-6. Table 2. 7 shows the payoff matrix and the parameters required for implementing the AUGMECON algorithm. Figure 2. 6-a shows the result of the AUGMECON algorithm used to solve the proposed MOMILP, considering each objective as the primary. Figure 2. 6-b magnifies the Pareto optimal solutions for the last four values of F1 (0.4, 0.6, 0.8, and 1.0) from Figure 2. 6-a. As shown in Figure 2. 6-a (and Figure 2. 6-b), the

epidemiological impact (F1) and the economic impact on local businesses (F3) are negatively correlated. As more states open local activities, the impact on local businesses decreases while the number of patients increases. While the model tries to minimize the adverse economic impact on trade (F2), it opens more industries in each city, which will increase the number of infected employees, thereby increasing the number of infections.

In scenario 4, the epidemiological and economic impacts on trade are positively correlated. Therefore, the model tries to decrease the economic impact on trade by keeping more industries open (tradable industries, K_1, and non-tradable industries, K_2). However. since opening states and all industries would significantly increase the number of patients, the model chooses to close more states and less demanded local industries, so the economic impact on trade would be minimized.

Therefore, the feasible solution region and the Pareto-optimal solutions for the MOMILP show a convex and nonlinear behavior. Deriving the Pareto-optimal solutions for the convex and nonlinear multi-objective functions using other approaches is adequately addressed in the literature (Das & Dennis, 1998; Hartikainen et al., 2012). In this example, the optimality gap equals 5%, and all the Pareto solutions are non-dominated.

Table 2. 7. The normalized payoff matrix and range of three objective functions

	$F1$ value	$F2$ value	$F3$ value
Min $F1$	0.000	1.000	1.000
Min $F2$	1.000	0.000	0.813
Min $F3$	0.668	0.973	0.000

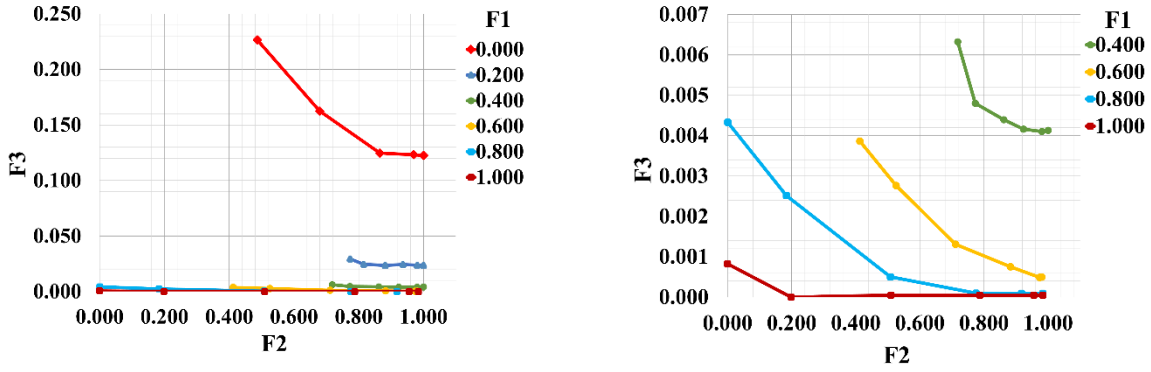

(a) ***(b)***

Figure 2. 6. The results of the proposed MOMILP for Scenario 4 consider (a) full grid Pareto optimal solutions, (b) selected 24 Pareto optimal solutions with the value of F1 equal to 0.4, 0.6, 0.8, 1.0.

For each scenario presented in Table 2. 6, we measure the value of the three objective functions, including the average percentage of patients (F1), the average trade impact (F2, measured by the percentage of unmet demand), and the average local businesses impact (F3, measured by the percentage of business shrinkage). For the sake of compression of the four scenarios, we choose a solution from the Pareto-optimal solutions set that results in the minimum cubic distance from the lower bound of each objective in that specific scenario. For instance, among the 36 Pareto-optimal solutions obtained for scenario 4, one of the solution points has the lowest cubic distance with the minimum values of F1, F2, and F3 from the payoff matrix. The selected Pareto solution results in the normalized values of the three objective functions such that F1= 0.692, F2=0.918, and F3=0.000.

The first three scenarios focus on minimizing only one objective. Therefore, the average percentage of patients, the average percentage of local business shrinkage, and the average percentage of unmet demand are minimum in scenarios 1, 2, and 3, respectively. The results obtained from scenario 4 show significantly different outcomes. In this scenario, the

optimum values of each objective are roughly close to each other, while in the first three scenarios, the range of each objective is significantly higher. The Pareto-optimal solutions suggest that for any control decision (state and industry closure or reopening), the economic and epidemiological impacts change in the opposite direction. At the same time, it is more effective to close most states and keep the majority of industries open .The MOMILP model tries to minimize one objective while considering the possible optimum value of the other objectives. Therefore, the results from all three MOMILP objective functions are more convincing for decision-makers interested in minimizing all three aspects of the pandemic impact. The selected Pareto solution suggests opening more industries to minimize the significant economic impact on trade rather than closing more states. The results show that the economic impact of industries and state closure overcome the epidemiologic impact in terms of the number of infected people. However, this result is not reflecting the economic impact of the increase in the number of infected people, including the healthcare costs and workforce loss.

Figure 2. 7 shows the optimum value of each objective changing over the time horizon of $T = 10$ for each of the four scenarios presented in Table 2. 6. Results for scenario 4 belong to the selected solution among the Pareto optimal solutions set, with the minimum cubic distance from the lower bound of F1, F2, and F3. As shown in Figure 2. 7a, objective function Min F1 in scenario 1, decreases the percentage of patients quickly as the model forces more states and industries to be closed. This decrease results in a higher economic impact on local businesses and trade, as shown in Figure 2. 7b and Figure 2. 7c. With objective function Min F2 in scenario 2, the percentage of patients decreases more slowly than in scenario 1 as scenario 2 minimizes the economic impact on local businesses by closing fewer states. While

fewer states and local businesses are closed, to keep the number of patients lower than its upper bound, the model closes more industries, leading to an increased impact on trade. Objective function Min F3 in scenario 3 minimizes the economic impact on trade, so it tries to keep more industries open. Since open industries result in higher employee infection, the model forces more states to close to keep the number of infections lower than its upper bound. In this case, the economic impact on local businesses is higher than in scenario 2, while the number of patients is less. The three single objective function scenarios result in extreme points of each objective function without considering the importance of other objectives. In contrast, the MOMILP objective functions in scenario 4, generally result in an average solution that considers the importance of all objectives.

As shown in Figure 2. 7b, the percentage of patients decreases over time, as all MOMILP models force more states to close. All MOMILP models keep more industries open since they value the economic impact on trade. Therefore, the range of economic impact is significantly lower than in the first three scenarios. The MOMILP models balance the epidemiological impact and the economic impact while considering the importance of their specific objective function as a priority. In the selected Pareto-optimal solution sets in scenario 4, the epidemiological impact and economic impacts oscillate during the time horizon as the MOMILP models give a different sequence of opening and closure. In scenario 4, the average local business impact increases, as more states are closed, and to decrease the economic impact on trade, more industries are opened. As shown in Figure 2. 7c, the epidemiological impact in the three MOMILP models in scenario 4 is decreasing with closer values than in scenarios 1, 2, and 3

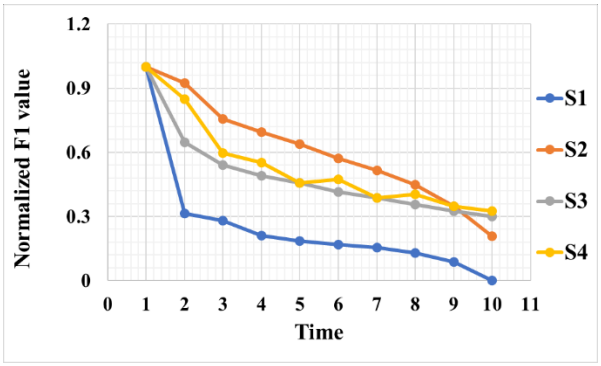

(a)

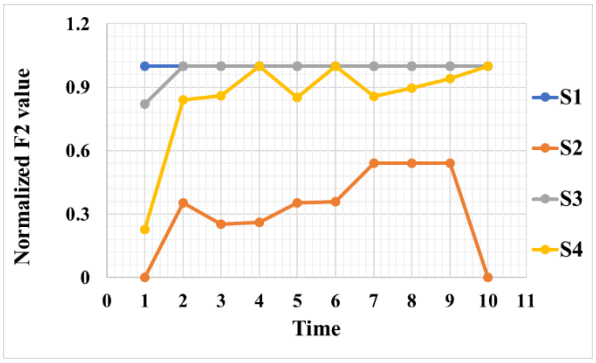

(b)

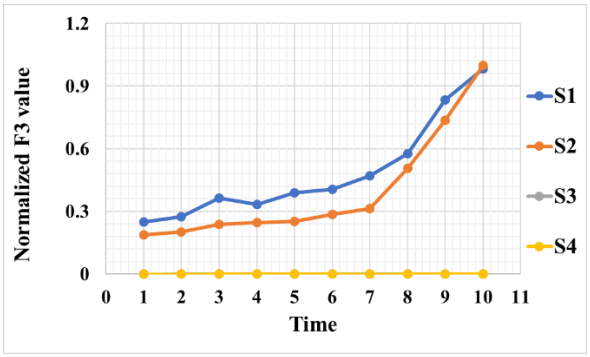

(c)

Figure 2. 7. The results of the proposed model for (a) average percentage of patients in scenarios 1-4, (b) average percentage of local business impact in scenarios 1-4, and (c) average percentage of trade impact in scenarios 1-4.

Finally, each optimal solution controls policies over the considered time horizon. Figure 2. 8 shows the optimal opening and closure policy for each state and industry over the time horizon and scenarios 1-4. All the policies regarding the opening and closure of states and industries comply with the results explained in Figure 2. 7. The more industries in each state

that are closed, the more unmet demand for the product of those industries increases in the same state and the other states. The MOMILP models in scenario 4 keep the balance of all three objectives. The MOMILP models mostly keep more industries open to decrease the unmet demand, while they keep more states closed to decrease the percentage of patients.

In contrast, the results of scenarios 1-3, where each scenario only considers one objective function, are significantly different. For example, the comparison of Scenario 1 and scenario 4, shows how scenario 1 keeps the number of patients minimum (F1 is the objective function in scenario 1) and scenario 4 tries to keep the number of patients as minimum as possible. At the same time, it also tries to minimize the two economic impacts.

Moreover, the industry status is decided based on the amount of trade between states for a specific commodity. In MOMILP majority of industries are open due to the high economic impact their closure may cause. The industries that are closed more often are located in the District of Columbia. According to Figure 2. 5, the District of Columbia mainly supplies a small number of commodities, mainly from the *Wholesale trade* and *Manufacturing* industries. The *Wholesale trade* industry is closed at time 5, while the *Manufacturing*, *Mining*, *Retail trade*, *Information*, and *Management* industries are closed during the whole planning horizon. In Vermont, where the export of commodities is lower, *Retail trade*, *Warehouse and storage*, and *Information* industries are closed at times $t =$ Error! Bookmark not defined., $t = \{1{:}\,9\}$, and $t = \{5,6,8,9\}$ respectively.

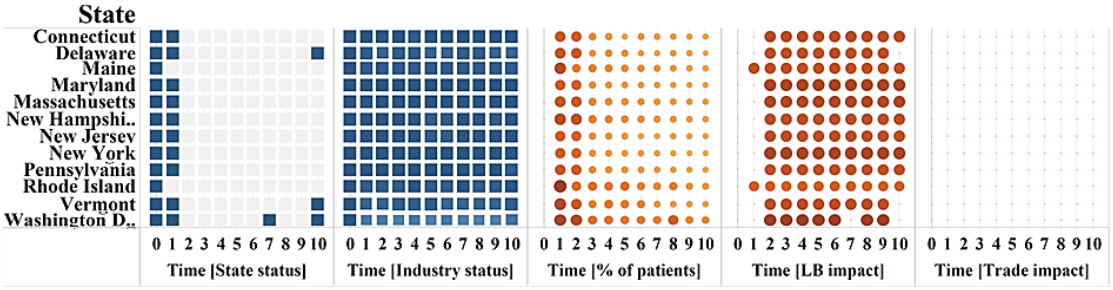

(a) Pandemic policy in scenario 1

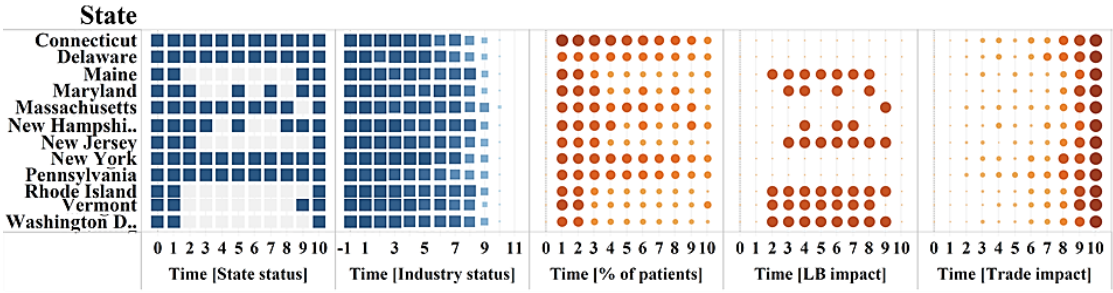

(b) Pandemic policy in scenario 2

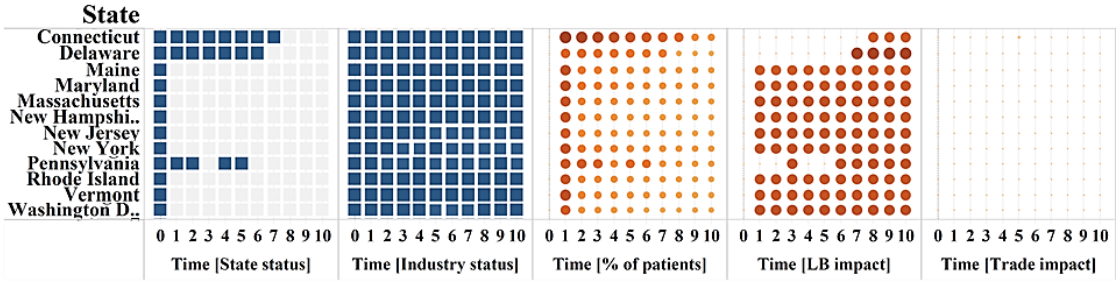

(c) Pandemic policy in scenario 3

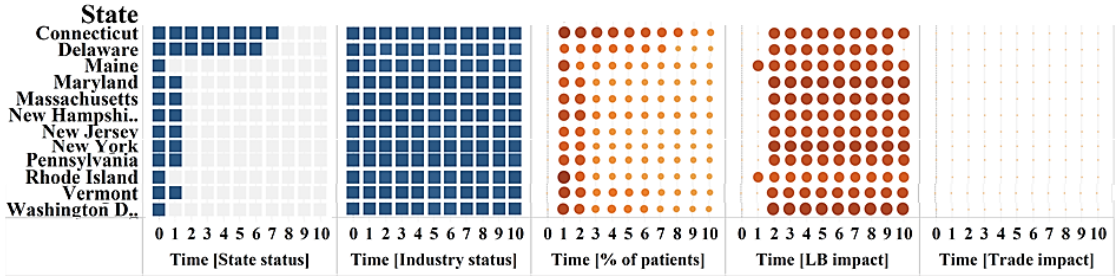

(d) Pandemic policy in scenario 4

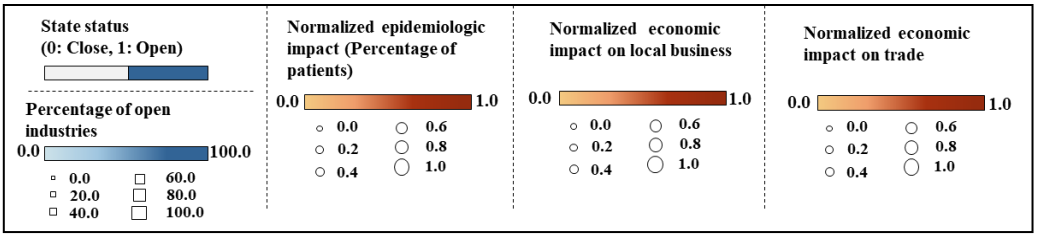

Figure 2. 8. Closure and reopening policies at the state and industry level over the time horizon of $T = 10$ in scenarios 1-4.

The other industries are closed accordingly. In New York, which has the second-highest export value, the *Transportation* and *Accommodation* industries are closed at time $\boldsymbol{t} = \{\mathbf{5}\}$ and $\boldsymbol{t} = \{\mathbf{3}\}$ respectively. In Maryland, *Manufacturing* is closed at time $\boldsymbol{t} = \{\mathbf{6}\}$, and in Delaware and Maine, the *Management* industry is closed at times $\boldsymbol{t} = \{\mathbf{1}\text{:}\mathbf{10}\}$ and $\boldsymbol{t} = \{\mathbf{5}\}$, respectively. Results show that the economic impact on trade is significantly important, and therefore the important industries with high traded values in specific states (e.g., *Manufacturing*, *Wholesale trade*, *Warehouse, and storage*) are staying open more often during the planning horizon.

2.5. Model Efficiency

The most influential input parameter on the efficiency of the proposed model is the time horizon, *T*. Figure 2. 9 shows the efficiency of the objective functions (scenarios 1, 2, and 3) for the planning time horizon of 1 to 12 units of time intervals (10 days). Figure 2. 9 suggests that increasing the time horizon will result in a linear increase in the number of decision variables. However, it exponentially increases the computational time.

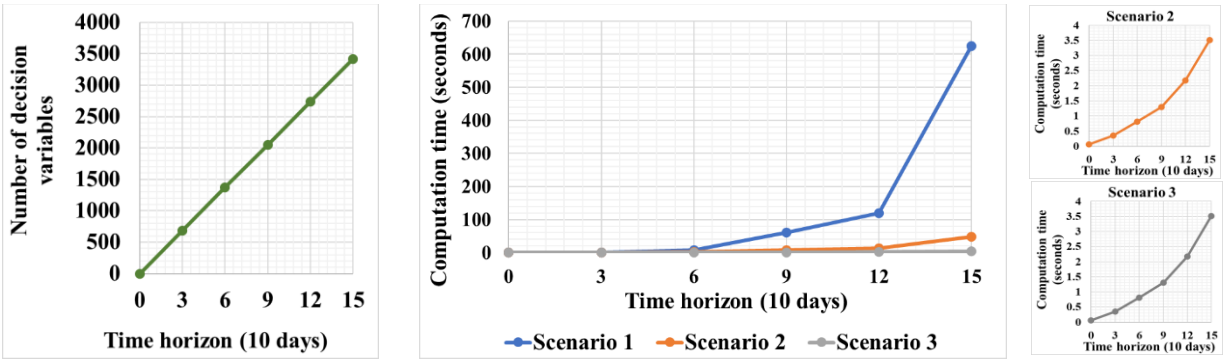

Figure 2. 9. The number of variables and the computational time for scenarios 1-3.

2.6. Concluding Remarks

This research explores a practical decision-making tool that can improve state-level and industry-level operational decisions during pandemic outbreaks. We propose a novel decision framework that integrates SIRD, MNFP models, and unemployment measures into mixed-integer linear programming for estimating the best control strategy over a specified time horizon. The contribution of this paper lies in (i) accounting for the two-fold economic (supply and demand perturbation and the raised unemployment) and epidemiological mechanisms of the pandemic, simultaneously, (ii) incorporating the interdependency between industry and state-level pandemic-driven decisions, and (iii) providing a decision support tool for optimizing the closure and reopening strategies during the pandemic planning period.

The proposed framework minimizes three main components: (i) the economic impact on the supply and trade equilibrium measured by the MNFP formulation, (ii) the economic impact on local businesses based on their unemployment rate, and (iii) the epidemiological impact based on the number of the infected population measured by SIRD formulation. While the reopening of the industries decreases the negative economic impact, it also contributes to increasing the number of the infected population. Also, the state reopening contributes to the number of infected populations, which ultimately impacts the workforce effectiveness of the industries, and finally, it impacts the economy of the states. Therefore, the timing and the choice of closure and reopening of states and industries are important for minimizing both the economic and the epidemiological impact of the pandemic.

The proposed model is implemented on the COVID-19 data over 11 states, the District of Columbia, and 19 industries in the US. The results show that with a different combination of economic and epidemiologic components, some states have shown a high percentage of patients in some scenarios while others have shown a high level of negative economic impact. Furthermore, the closure of each industry in one state may affect the unmet demand in another state and therefore affect the closure or opening of industries in the same or other states. The proposed MOMILP result in more state closure rather than industry closure. Three large states such as New York, New Jersey, Massachusetts, and Maryland, are closed more often, while the high economic impact on local businesses keeps Pennsylvania, Connecticut, and Delaware open more often. District of Columbia has small sizes of industries that have small contribution to supply for the demand and have less export to the other states; therefore, those industries are closed more often. The industries that are closed more often include *Management*, *Information*, *Retail trade*, *Mining*, and *Manufacturing*, mostly in the District of Columbia, Vermont, and New York. The reason for the closure of these industries in a specific state is the low output level that they have.

While temporal state-level and industry-level policies are vital for controlling the early stage impacts of the pandemic, several other impacts need to be considered in the later stage decisions. It has been proven that a pandemic's epidemiological and economic impact propagates to the other aspects of life, including socio-demographic vulnerabilities, perception of social equity in access to resources, fair vaccination distribution, and community-level job loss vulnerability, among others. On the other hand, the scale of closure and reopening, specific to each state and each industry in each state, significantly affects the efficiency of control strategies.

As such, future work will explore (i) quantifying the direct effect of business and industry closure in one state on the business and industry in other states (i.e., multi-regional interdependent economic impacts), (ii) incorporating various levels of the strictness of the control policy based on the criticality of industries, businesses, and states, (iii) incorporating the fairness of the controlling policy based on social vulnerabilities of infection, death, job losses, and accessibility to the resources, among others, and (iv) measuring the effect of the adoption and the timing of vaccination on the optimal closure and reopening strategies.

Chapter 3: MULTI-REGIONAL, MULTI-INDUSTRY IMPACTS OF FAIRNESS ON THE PANDEMIC POLICIES

3.1. Introduction

Sudden Acute Respiratory Syndrome – Coronavirus-2 (SARS-Cov-2), which produces the resulting disease of COVID-19, was declared a pandemic by the World Health Organization (WHO) on January 9, 2020 (Organization, 2020). In the US, COVID-19 had its first confirmed case in Washington State on January 19, 2020 (Zimmermann et al., 2020) and until now there have been various waves of growth in several infections and deaths. Since the beginning of the pandemic, different states, counties, and municipalities around the country implemented various strategies to control the spread of the virus (Chowell & Mizumoto, 2020). According to the previous studies, lockdown and quarantine policies diminish the number of infected, hospitalized, and deceased cases. However, such policies also decrease the economic output of the closed industries, which leads to a disastrous cascading effect across other industries in the state where the strategy is enacted as well as in other states. On the other hand, opening states and industries may increase the risk of growth in infected, hospitalized, and deceased cases. Therefore, the main dilemma would be identifying an optimal control strategy and the time when it should be implemented such that the pandemic-related effects are minimized while maintaining some level of economic, health, and societal equity (Andersen et al., 2020; Ocampo & Yamagishi, 2020; Pronk & Kassler, 2020).

Lockdowns and business shutdowns in various states have also led to business closures, increased unemployment (Blustein et al., 2020), and workforce losses in critical businesses

(Blustein & Guarino, 2020), and a lack of supply produced by specific industries (Chowell & Mizumoto, 2020). According to the Bureau of Labor Statistics (Bureau of Labor Statistics, 2022), the US unemployment rate was 3.6% pre-COVID and it increased to 15% in May 2020. Several studies addressed the short-term and long-term employment impact of the COVID-19 crisis (Cohen, 2020; Fana et al., 2020). Besides the fact that the infection and death rate has been different in each state, the change in the rate of unemployment, however, has not been the same over the states and industries. Therefore, due to the different socio-economic attributes of each state, the controlling policy should be adjusted to the important attributes of each state and each industry to keep fairness between states, and between industries.

When it comes to healthcare, fairness is not only defined as equity, but it means avoiding discrimination against social communities in different states and employees of different industries. There is a disparity among races in their vulnerability to COVID-19 infection, hospitalization, and death (Bureau of Labor Statistics, 2022). Also, certain industries have experienced more job losses. The importance of considering social fairness in determining pandemic policy has been studied in recent research (Buso et al., 2020; Martins-Filho et al., 2021; Paton, 2020). Social fairness in the decision process can include considering the demographic attributes of the communities in each state and demographic attributes of the employees in each industry, such as age, race, and gender, among others. It also stems from considering the socio-economic attributes of the affected population such as their wealth and their accessibility to healthcare services and equipment, among others (Newdick et al., 2020; White & Angus, 2020). Therefore, deriving a comprehensive policy to control the spread of the pandemic as well as controlling the effects of the pandemic requires consideration of social fairness.

Closing industries have had a significant impact on the economy by disturbing the supply and demand equilibrium (Pichler & Farmer, 2021). According to the input-output economic model, each industry's commodity is consumed either by the final consumer or used by other industries to produce another commodity (Leung et al., 2007). Therefore, when infections cause labor loss in an industry, the supply capacity in that industry decreases, and the lack of supply propagates to the other interdependent industries in the same states (Yu & Aviso, 2020). Designing a control policy that minimizes such industry inoperability is critical for reducing negative economic impacts. State closures or lockdowns during the pandemic have also decreased the demand for certain industries such as entertainment, hotel, and dining industries, among others. The decrease in demand also can affect the economic system balance, however, in this study, we are only considering the industry closure and supply-side effect of the pandemic.

The application of the input-output (I-O) economic model to analyze the cascading economic effects of disruptive events has been studied for a wide variety of domains (Galbusera & Giannopoulos, 2018; Li et al., 2017), including the COVID-19 pandemic (Galbusera & Giannopoulos, 2018; Sarmidi et al., 2021; Socci et al., 2021). Hishikar (2021) estimate the impact of the COVID-19 pandemic on India's economy using the inoperability input-output model (IIM), estimating a 4.2% in the output of transport and hotel industries due to the complete lockdown. Yu et al. (2020)studied the effect of extended shutdown of business operations using a persistent inoperability input-output model (PIIM), showing that industries with higher levels of inoperability would recover faster and initially unaffected industries would experience inoperability levels higher than directly affected industries over time. Santos (2006)explored the impact of pandemics on the workforce with

several mitigation and suppression policies using an I-O framework. Richiardi et al. (2020) analyzed the effects of the COVID-19 lock-down on final demand and supply in key industries in the UK using a dynamic I-O model that allows for both demand-side and supply-side perturbations. Chen et al. (2021) combined an epidemiological model describing the spread of COVID-19 with an I-O model to measure the direct and indirect impacts of labor supply shock on each industry. Results indicated that the trade-offs between economic losses and the epidemiologic impact of the pandemic is non-linear with respect to social distancing and lockdown duration decisions. Also, industries relying on physical labor, such as the Agriculture and Construction industries, were more adversely impacted by the pandemic compared to those industries that rely on professional labor services.

Since the evolution of the COVID-19 pandemic, various research studies have analyzed the pandemic's social, economic, and epidemiologic impacts at international and national levels, as well as providing a wide range of policies to mitigate the crisis effect of this pandemic (Brodeur et al., 2020; Gros & Gros, 2021; Jackson et al., 2020; Nicola et al., 2020; Ocampo & Yamagishi, 2020; Principato et al., 2020; Soufi et al., 2022). The majority of the available literature has prescribed control strategies based on a descriptive analysis of the available epidemiologic and economic statistics (Balla-Elliott et al., 2020; Seyedin et al., 2020; Wang et al., 2020). However, to the best of the authors' knowledge, no published work has proposed a mathematical model to simulate the effect of control policies and identify the optimal closure and reopening strategies at the state and industry levels during a specific timeline of planning. This research presents multiple contributions to the literature, including (i) proposing a prescriptive decision-making tool based on a multi-objective mixed-integer linear programming optimization model that results in an optimal policy to

control the pandemic at the state and industry level, (ii) proposing a decision-making model that incorporates the societal fairness, epidemiologic impact, and the inoperability impact of the pandemic in deriving the optimal control policy, (iii) considering the social fairness attribute from two aspects including the vulnerability of communities to both getting infected by COVID-19 due to state opening decisions and losing employment due to state closure decisions, measured by the deviation from a national social vulnerability index, and (iv) quantifying the inoperability impact of a pandemic by combining the supply side multi-regional inoperability input-output model (MRIIM) and the industry level decisions within the optimization model. It is assumed that all companies within an industry behave the same way.

3.2. Problem Formulation

This section provides the methodological background of the MRIIM and SIRD models, as well as the proposed mathematical model for providing the optimal state- and industry-level pandemic policies that balances the social, economic, and epidemiological impacts of the pandemic. Also, social fairness is quantified as the numerical deviation of the social vulnerability of each state from the average national vulnerability index at each period during the planning horizon. The model results in the optimal closure and reopening strategies for (i) each industry, (ii) each state, and (iii) each period, along with the three impacts of each decision. With such an optimization framework, we look to address different decision-making perspectives: state-level decisions, national-level decisions, industry-level decisions, and how any of these trade-offs with each other.

3.2.1. Multi-Regional Inoperability Input-Output Model

The basic economic input-output model (Leontief, 1986) assumes that the economy consists of a group of n interacting industries, each producing a single commodity. Therefore, under a static equilibrium of the economy, the total output of each industry is distributed to all industries and satisfies external demand. This is represented in Eq. (3. 1), where the output from industry i, x_i, is equal to the sum of output flows, z_{ij}, from industry i to j and the external demand, c_i, industry i. That is, the total output from industry i is found from (i) the intermediate demand required for production in other industries and (ii) the amount demand directly by consumers. Flow z_{ij} can be rewritten as the product of the proportional requirement, a_{ij}, of industry i output to industry j's output and the output of industry j, x_j. Proportional coefficient a_{ij} is called the Leontief coefficient or technical coefficient.

$$x_i = \sum_{j=1}^{n} z_{ij} + c_i = \sum_{j=1}^{n} a_{ij}\, x_j + c_i \qquad (3.\ 1)$$

Eq.(3. 1) can be written in a matrix form as in Eq.(3. 2), where $\mathbf{x}$ is an $n \times 1$ vector of industry outputs, $\mathbf{c}$ is the $n \times 1$ vector of the final industry demand, and $\mathbf{A}$ is the $n \times n$ matrix of technical coefficients.

$$\mathbf{x} = \mathbf{A}\mathbf{x} + \mathbf{c} \qquad (3.\ 2)$$

To regionalize the input-output model, the elements of the $\mathbf{A}$ matrix are modified to form the regional input-output matrix $\mathbf{A}^r$ in Eq.(3. 3) (Miller & Blair, 2009), where l_i is the location quotient and is an indicator of the extent to which industry i is used in the output of industry j in region r.

$$a_{ij}^{r} = \begin{cases} l_i a_{ij} & l_i < 1 \\ a_{ij} & l_i \geq 1 \end{cases} \tag{3. 3}$$

Location quotient l_i is calculated in Eq.(3. 4), where x_i^r is the output of the industry i in region r, x_{total}^r is the total output of industries in region r, x_i is the total output of industry i, and x_{total} is the total output of all industries at the national level.

$$l_i = \frac{x_i^r / x_{total}^r}{x_i / x_{total}} \tag{3. 4}$$

Therefore, the multi-regional input-output model for the p regions can be written as Eq. (3. 5).

$$\begin{bmatrix} \mathbf{x}^1 \\ \mathbf{x}^2 \\ \vdots \\ \mathbf{x}^p \end{bmatrix} = \begin{bmatrix} \mathbf{A}^1 & 0 & \cdots & 0 \\ 0 & \mathbf{A}^2 & & 0 \\ \vdots & & \ddots & \vdots \\ 0 & 0 & \cdots & \mathbf{A}^p \end{bmatrix} \begin{bmatrix} \mathbf{x}^1 \\ \mathbf{x}^2 \\ \vdots \\ \mathbf{x}^p \end{bmatrix} + \begin{bmatrix} \mathbf{c}^1 \\ \mathbf{c}^2 \\ \vdots \\ \mathbf{c}^p \end{bmatrix} \tag{3. 5}$$

Isard et al. (2017) proposed an extended model for incorporating the inter-regional trade and commodity flows in the input-output model calculations. Eq.(3. 6) shows the basis for the inter-regional input-output flow model, where t_i^{rs} is the proportion of commodity i consumed by region s that originated in region r.

$$a_{ij}^{rs} = t_i^{rs} a_{ij}^{r} \tag{3. 6}$$

The inter-regional input-output model can then be summarized in Eq.(3. 7), where each sub-matrix $\mathbf{T}^{rs}$ is an $n \times n$ diagonal matrix whose diagonal elements are t_i^{rs} values.

$$\begin{bmatrix}\mathbf{x}^1\\ \mathbf{x}^2\\ \vdots\\ \mathbf{x}^p\end{bmatrix}=\begin{bmatrix}\mathbf{T}^{11} & \mathbf{T}^{12} & \cdots & \mathbf{T}^{1p}\\ \mathbf{T}^{21} & \mathbf{T}^{22} & & \mathbf{T}^{2p}\\ \vdots & & \ddots & \vdots\\ \mathbf{T}^{p1} & \mathbf{T}^{p2} & \cdots & \mathbf{T}^{pp}\end{bmatrix}\begin{bmatrix}\mathbf{A}^1 & 0 & \cdots & 0\\ 0 & \mathbf{A}^2 & & 0\\ \vdots & & \ddots & \vdots\\ 0 & 0 & \cdots & \mathbf{A}^p\end{bmatrix}\begin{bmatrix}\mathbf{x}^1\\ \mathbf{x}^2\\ \vdots\\ \mathbf{x}^p\end{bmatrix} \quad (3.\ 7)$$

$$+\begin{bmatrix}\mathbf{T}^{11} & \mathbf{T}^{12} & \cdots & \mathbf{T}^{1p}\\ \mathbf{T}^{21} & \mathbf{T}^{22} & & \mathbf{T}^{2p}\\ \vdots & & \ddots & \vdots\\ \mathbf{T}^{p1} & \mathbf{T}^{p2} & \cdots & \mathbf{T}^{pp}\end{bmatrix}\begin{bmatrix}\mathbf{c}^1\\ \mathbf{c}^2\\ \vdots\\ \mathbf{c}^p\end{bmatrix}$$

The basic formulation of the Multi-Regional Inoperability Input-Output Model (MRIIM), shown in Eq.(3. 8), has foundations in the input-output model but where, rather than traditional commodity flows, the propagation of inoperability among industries in different regions is studied. Inoperability can be thought of as the proportional extent to which industries are not productive due to a direct or interdependent disruption (Santos, 2006). Inoperability is measured with vector $\mathbf{q}$. Vector $\mathbf{c}^*$ is a vector of direct perturbation to an industry's production, $\mathbf{T}^*$ is the $n \times n$ normalized diagonal regional trade coefficient matrix, and $\mathbf{A}^*$ is the $n \times n$ normalized matrix of technical coefficients. (Miller & Blair, 2009).

$$\mathbf{q} = \mathbf{T}^*\mathbf{A}^*\mathbf{q} + \mathbf{T}^*\mathbf{c}^* \;\Leftrightarrow\; q_i^r = \sum_{s=1}^{p}\sum_{j=1}^{n} t_i^{*rs} a_{ij}^{*s} q_j^s + \sum_{s=1}^{p} t_i^{*rs} c_i^{*s} \quad (3.\ 8)$$

The formulations for q_i^r, c_i^{*s}, $\mathbf{A}^*$ and T^* are presented in Eq.(3. 9)-(3. 12) respectively, where diag($\mathbf{x}$) is the diagonal matrix formed by the industry output vector.

$$q_i^r = \frac{as\ planned\ output\ (x_i^r) - Perturbed\ output\ (\tilde{x}_i^r)}{as\ planned\ output\ (x_i^r)} \Leftrightarrow \mathbf{q} = \mathrm{diag}(\mathbf{x})^{-1}\,\Delta\mathbf{x} \quad (3.\ 9)$$

$$c_i^{*s} = \frac{as\ planned\ demand\ (c_i^r) - Perturbed\ demand\ (\tilde{c}_i^r)}{as\ planned\ output\ (x_i^r)} \Leftrightarrow \mathbf{c}^* = diag(\mathbf{x})^{-1}\,\Delta\mathbf{c} \quad (3.\ 10)$$

$$\mathbf{A}^* = \mathrm{diag}(\mathbf{x})^{-1}\,\mathbf{A}\,\mathrm{diag}(\mathbf{x}) \quad (3.\ 11)$$

$$\mathbf{T}^* = \mathrm{diag}(\mathbf{x})^{-1}\,\mathbf{T}\,\mathrm{diag}(\mathbf{x}) \quad (3.\ 12)$$

The MRIIM is developed to help understand the interdependencies between regional and inter-regional perturbations in different industries. The original model is demand-driven, wherein final demand perturbations impact the production outputs of different interdependent industries from the direct and indirect effects. (Leung et al., 2007) extended the IIM with supply-side and output-side effects. The output-side IIM model measures the impact of direct perturbation on the output of an industry, which could have been caused by capacity loss, facility closure, or supply flow disruption, among others. Such disruptions are turned into a direct reduction in the output level of the interdependent industries. In this case, the MRIIM model can be revised to handle mixed exogenous (demand or supply) and endogenous (output) specified variables (Leung et al., 2007).

In general, assuming that among n industries, r ($r \leq n$) industries are disrupted and have exogenously determined output, then the inoperability vector can be divided into two sets, q and $\bar{q}$, where q is the inoperability vector of $(n - r)$ industries, whose values are to be determined by the model, and $\bar{q}$ is the inoperability vector of the r industries, whose values are exogenously specified. For the disrupted industries, the final demand perturbation vector should be determined by the model ($\bar{c}^*$) and for the remaining $(n - r)$ industries, the final demand perturbation vector is exogenously specified (c^*). Therefore, by rearranging Eq. (3. 8), the value of exogenous inoperability and the final demand can be determined in Eq.(3. 13) (Crowther & Haimes, 2010), and the linear formulation can be presented in Eq.(3. 14).

$$[I - T^* A^*] \begin{bmatrix} q \\ \bar{q} \end{bmatrix} = [\, T^*] \begin{bmatrix} \bar{c}^* \\ c^* \end{bmatrix} \tag{3. 13}$$

$$(1 - t_i^{*rr} a_{ii}^{*r}) q_i^r - \sum_{s=1}^{p} \sum_{\substack{j=1 \\ i \neq j}}^{n} t_i^{*rs} a_{ij}^{*s} q_j^s = \sum_{s=1}^{p} t_i^{*rs} c_i^{*s} \quad (3.14)$$

Without loss of generality, Eq.(3. 8) can be used in the mathematical optimization models where q and c can be either a parameter (exogenously specified) or a decision variable (indigenously specified in the model).

3.2.2. Modified SIRD Model

The susceptible-infected-recovered-deceased (SIRD) model is a well-known mathematical representation of the dynamics of an epidemic or a pandemic (Zhu et al., 2019). The formulation of the SIRD model used in this research is resented in section 2.2.2. is governed by ordinary differential equations or fractional differential derivatives (Kermack & McKendrick, 1927). It formulates the relation between the numbers of susceptible cases $S(t)$, infected cases $I(t)$, recovered cases $R(t)$, and deceased cases $D(t)$ at each time and in a certain population.

3.2.3. Proposed mathematical model

The proposed model combines the Multi-Regional Inoperability Input-output model and the modified SIRD model to optimize the timing of the implementation of control strategies at the industry and regional levels. The definition of sets and the notation of the parameters and decision variables are shown in Table 3. 1, Table 3. 2, and Table 3. 3, respectively.

Table 3. 1. Model indices and sets

Set	Definition
N	Set of all states indexed by $i \in N$ and $j \in N$ (e.g., state 2)
K	Set of all industries indexed by $k \in K$.

Table 3. 2. Model parameters.

Parameters	Definition
α_i	The infection rate in state i
β^k	The infection rate in industry k
ρ	The recovery rate in the country
γ_i	The death rate in state i
π_i	The initial susceptible population in state i (equal to the initial population of state i)
h_i	The initial number of patients in state i
g_i	The initial status of the state i
f_i^k	The initial status of the state i for industry k
e_i^k	The initial number of employees in state i for industry k
q_{it}^k	Inoperability of industry $k \in K$ in state i due to its closure
x_{ij}^{*k}	Normalized amount of trade of industry $k \in K$ between state i and state j
a_i^{*lk}	Normalized amount of requirement of industry $l \in K$ from industry $k \in K$ in state i
d_i^{*k}	Normalized changes of final demand from industry $k \in K$ in state i
λ_i	Vulnerability of state i in regard to COVID infection
ξ_i	Index of the communities' job insecurity in state i due to pandemic policy
t_R	The average recovery period (~ 4 weeks)
t_I	The average immunity period (~ 12 weeks)
t_D	The average death period (~ 2 weeks)
m	Large number
t	The index of time ranging from 1 to time horizon T

Table 3. 3. Model decision variable.

Variable	Definition
q_{it}^{k}	The measure of the inoperability of industry $k \in K$ in state i due to the closure of other industries, continuous
v_{it}^{k}	The inoperability in industry $k \in K$ in state i due to the closure of other industries, continuous
v_{it}^{k}	The potential inoperability in industry $k \in K$ in state i due to the closure of other industries, continuous
c_{it}^{*k}	The measure of the normalized changes of final demand from $k \in K$ in state i, continuous
b_{it}^{*k}	The potential measure of the normalized changes of final demand from $k \in K$ in state i, continuous
p_{it}	Number of patients in state i at time $t = 1, \dots, T$, integer
w_{it}	Number of new patients in state i at time $t = 1, \dots, T$, integer
s_{it}	Number of total susceptible people in state i at time $t = 1, \dots, T$, integer
r_{it}	Number of susceptible people to infection in state i at time $t = 1, \dots, T$, integer
o_{it}^{k}	Number of total susceptible employees in state i and industry k at time $t = 1, \dots, T$, integer
n_{it}^{k}	Number of total susceptible employees to infection in state i and industry k at time $t = 1, \dots, T$, integer
y_{it}^{k}	Equal to 1 if industry k in state i is open at time $t = 1, \dots, T$, binary
z_{it}	Equal to 1 if state i is open at time $t = 1, \dots, T$, binary
δ_{t}	Average national vulnerability at time $t = 1, \dots, T$, integer
ϑ_{it}	Measure of state i's vulnerability at time $t = 1, \dots, T$
μ_{it}^{-}	Negative slack for the deviation of state i's vulnerability from the average of the country at time $t = 1, \dots, T$
μ_{it}^{+}	Positive slack for the deviation of state i's vulnerability from the average of the country at time $t = 1, \dots, T$

The proposed multi-objective mixed-integer linear programming (MOMILP) model contains three distinct objective functions shown in Eqs. (3. 15)-(3. 17), including (i) the average epidemiological impact in terms of the percentage of the infected population across the states and over the time horizon of the decision-making (F1), (ii) the average social impact value of the controlling policy in terms of the deviation of the social vulnerability from the national average social vulnerability in state closure over the time horizon of the

decision making (F2), and (iii) the average economic impact of controlling policy in terms of the inter-regional inoperability measure across industries and states over the time horizon of the decision making (F3).

It is expected that the epidemiological impact (F1) and the economic impacts (F3) compete such that any strategy that decreases the epidemiological impact by industries closure would result in an increase in economic impact due to a higher inoperability, and vice versa. Also, the epidemiological impact (F1) and the social impacts (F2) may affect each other adversely if any strategy that decreases the epidemiological impact by state closure increases the social vulnerability deviation from the national average. Therefore, the MOMILP model balances all three objectives simultaneously.

Eq.(3. 18) measures the level of the inoperability where q and c can be either the decision variables or a parameter. If the industry *k* in state *i* is open ($y_{it}^{k} = 1$), then demand for the commodity of that industry is indigenously determined, and the inoperability level should be calculated exogenously based on the status of the interdependent industries. If the industry *k* in state *i* is closed ($y_{it}^{k} = 0$), then demand for the commodity of that industry is perturbed and should be calculated exogenously, while the inoperability level is defined indigenously as the result of the percentage of output loss. Eqs. (3. 19)-(3. 22) and Eqs. (3. 23)-(3. 26) are defined to determine whether q and c are decision variables or parameters based on the status of the industry (closed or open). For instance, if the industry *k* in state *i* is open ($y_{it}^{k} = 1$), then $q_{it}^{k} = v_{it}^{k}$ and $v_{it}^{k} = vv_{it}^{k}$ from Eqs.(3. 20)-(3. 21) and v_{it}^{k} is an unbounded decision variable in Eq. (3. 22). On the other hand if industry *k* in state *i* is closed ($y_{it}^{k} = 0$), then $q_{it}^{k} = u_{i}^{k}$ in Eq.(3. 19) and $v_{it}^{k} = 0$ from Eq.(3. 22) while vv_{it}^{k} is a positive

decision variable which will not affecting the MRIIM model. The same explanation is applicable to Eqs.(3. 23)-(3. 26).

Eqs. (3. 27)-(3. 29) quantifies the social vulnerability value coming out of the controlling policy at the state level. Two indicators are defined for the social vulnerability index, including (I) COVID-19 Community Vulnerability Index (CCVI), ξ_i, in state *i*, and (II) the community job security during COVID-19, λ_i, in state *i*. The value of ξ_i measures the risk of getting COVID-19 in each state and it incorporates different factors, such as socioeconomic status, minority, and language status, household and transportation availability, epidemiological factors, healthcare system factors, the high-risk environment of living and working ad the population density. The data regarding the ξ_i is determined by the COVID Community Vulnerability Index (CCVI) measured by (Surgo Ventures, 2021a). The value of λ_i is measured by incorporating the size of each industry in each state and their associated employment change during Feb 2020- Feb 2021 by considering the type of industry and the community attributes of the employees such as age, gender, education level, and race and ethnicity. Eq.(3. 27)measures the social vulnerability index for each state at each time (ϑ_{it}) and Eq.(3. 28) measures the average social vulnerability index at the national level (δ_t). Eq.(3. 29) quantifies the deviation of the social vulnerability of each state from the national social vulnerability index, which can be a negative deviation (μ_{it}^-) or a positive deviation (μ_{it}^+). The summation of positive and negative deviation will be minimized in the second objective function.

Eqs. (3. 30)-(3. 44) generate the bounds for the modified SIRD model. The epidemiologic impact measures the number of infected people who are infected either in their social life or

during their work time. Constraint (3. 30) updates the number of patients at each time based on the number of patients in the previous period, the newly infected people (W_{it}), the number of recovered cases at the time $t - t_R$ and the number of deceased cases at the time $t - t_D$. Eq.(3. 31) updates the number of new infectious (patients) based on the status of industries and states. It is assumed that every susceptible person may become infected during their work life or social life (except during work hours). Eq.(3. 31) is formulated to avoid double counting an employee's chance of infection during their work life and social life. To incorporate the relationship between the status of the industries and states and the number of new patients in a linear formula, r_{it} and n_{it}^k are defined in Eqs.(3. 32)-(3. 35) and Eqs. (3. 36)-(3. 39) respectively, with the same logic that is explained for Eqs. (3. 19)-(3. 22) earlier. For example, if state *i* is open ($z_{it} = 1$) then based on Eqs.(3. 33)-(3. 34), $r_{it} = s_{it}$ and s_{it} is the number of infected people in state *i* at time *t* measured by Eq.(3. 32). On the other hand, if state *i* is closed ($z_{it} = 0$), then there is no new infection at time *t* in state *i,* therefore $r_{it} = 0$ from Eq.(3. 35), being used in Eq.(3. 33). The same logic can be used to quantify the new infections in industries measured by Eqs.(3. 36)-(3. 39).

Eqs. (3. 40)-(3. 42) limit the infected and susceptible populations in each state to its total population and the infected workforce of industry k in state i to its total number of employees. Eqs. (3. 43)-(3. 47) define the initial value for each decision variable at time $t = 0$, and Eqs.(3. 48)-(3. 52) denote the nature of decision variables.

$$\text{F1: min} \quad \sum_{t=1}^{T}\sum_{i\in N}\left(\frac{p_{it}}{\pi_i}\right)\left(\frac{1}{NT}\right) \tag{3.15}$$

$$\text{F2: min} \quad \sum_{t=1}^{T}\sum_{i\in N}\left(\frac{\mu_{it}^{-}+\mu_{it}^{+}}{|NT|}\right) \tag{3.16}$$

$$\text{F3: min} \quad \sum_{t=1}^{T}\sum_{i\in N}\sum_{k\in K}\left(\frac{q_{it}^{k}}{NTK}\right) \tag{3.17}$$

s. t.

$$q_{it}^{l} = \sum_{j\in N}\sum_{k\in K}\left(x_{ij}^{*l}\, a_j^{*lk} q_{jt}^{k}\right) + \sum_{j\in N}\left(x_{ij}^{*l} c_{jt}^{*l}\right) \qquad \forall i \in N, \forall\, l \in K,\ t = 1, \dots, T \tag{3.18}$$

$$q_{it}^{k} = v_{it}^{k} + \left(1 - y_{it}^{k}\right)u_i^{k} \qquad \forall i \in N, \forall\, k \in K,\ t = 1, \dots, T \tag{3.19}$$

$$v_{it}^{k} \le v_{it}^{k} + m(1 - y_{it}^{k}) \qquad \forall\, i\ \in N, \forall\, k \in K,\ t = 1, \dots, T \tag{3.20}$$

$$v_{it}^{k} \ge v_{it}^{k} \qquad \forall\, i\ \in N, \forall\, k \in K,\ t = 1, \dots, T \tag{3.21}$$

$$v_{it}^{k} \le m\, y_{it}^{k} \qquad \forall\, i\ \in N, \forall\, k \in K,\ t = 1, \dots, T \tag{3.22}$$

$$c_{it}^{*k} = c_{it}^{*k} + y_{it}^{k}\, d_i^{*k} \qquad \forall i \in N, \forall\, k \in K,\ t = 1, \dots, T \tag{3.23}$$

$$b_{it}^{*k} \le c_{it}^{*k} + m y_{it}^{k} \qquad \forall\, i\ \in N, \forall\, k \in K,\ t = 1, \dots, T \tag{3.24}$$

$$b_{it}^{*k} \ge c_{it}^{*k} \qquad \forall\, i\ \in N, \forall\, k \in K,\ t = 1, \dots, T \tag{3.25}$$

$$c_{it}^{*k} \le m\,(1 - y_{it}^{k}) \qquad \forall\, i\ \in N, \forall\, k \in K,\ t = 1, \dots, T \tag{3.26}$$

$$\vartheta_{it} = \xi_i(1 - z_{it}) + \lambda_i z_{it} \qquad \forall i \in N,\ t = 1, \dots, T \tag{3.27}$$

$$\delta_t = \frac{1}{N}\sum_{i\in N}\xi_i(1 - z_{it}) + \lambda_i z_{it} \qquad t = 1, \dots, T \tag{3.28}$$

$$\vartheta_{it} - \delta_t + \mu_{it}^{-} - \mu_{it}^{+} = 0 \qquad \forall i \in N,\ t = 1, \dots, T \tag{3.29}$$

$$p_{it} = p_{i(t-1)} + w_{i(t-1)} - \gamma_i w_{i(t-t_D)} - (1 - \gamma_i) w_{i(t-t_R)} \qquad \forall i \in N,\ t = 1, \dots, T \tag{3.30}$$

$$w_{it} = \alpha_i \left(r_{it} - \sum_{k \in K} n_{it}^k \right) + (1 - (1 - \alpha_i)(1 - \beta_i^k)) \sum_{k \in K} n_{it}^k \qquad \forall i \in N,\ t = 1, \dots, T \qquad (3.31)$$

$$s_{it} = s_{i(t-1)} + (1 - \gamma_i) w_{i(t-t_R-t_I)} - w_{i(t-1)} \qquad \forall i \in N,\ t = 1, \dots, T \qquad (3.32)$$

$$s_{it} \leq r_{it} + m(1 - z_{it}) \qquad \forall i \in N,\ t = 1, \dots, T \qquad (3.33)$$

$$s_{it} \geq r_{it} \qquad \forall i \in N,\ t = 1, \dots, T \qquad (3.34)$$

$$r_{it} \leq m\, z_{it} \qquad \forall i \in N,\ t = 1, \dots, T \qquad (3.35)$$

$$o_{it}^k = o_{i(t-1)}^k - (1 - \gamma_i)\, \beta_i^k n_{i(t-t_R-t_I)}^k - \beta_i^k n_{i(t-(t_R+t_I))}^k \qquad \forall i \in N, \forall k \in K,\ t = 1, \dots, T \qquad (3.36)$$

$$o_{it}^k \leq n_{it}^k + m(1 - y_{it}^k) \qquad \forall i \in N, \forall k \in K,\ t = 1, \dots, T \qquad (3.37)$$

$$o_{it}^k \geq n_{it}^k \qquad \forall i \in N, \forall k \in K,\ t = 1, \dots, T \qquad (3.38)$$

$$n_{it}^k \leq m\, y_{it}^k \qquad \forall i \in N, \forall k \in K,\ t = 1, \dots, T \qquad (3.39)$$

$$p_{it} \leq \pi_i \qquad \forall i \in N,\ t = 1, \dots, T \qquad (3.40)$$

$$s_{it} \leq \pi_i \qquad \forall i \in N,\ t = 1, \dots, T \qquad (3.41)$$

$$o_{it}^k \leq e_i^k \qquad \forall i \in N, \forall k \in K,\ t = 1, \dots, T \qquad (3.42)$$

$$s_{it} = r_{it} = \pi_i \qquad \forall i \in N,\ t = 0 \qquad (3.43)$$

$$o_{it}^k = n_{it}^k = e_i^k \qquad \forall i \in N, \forall k \in K,\ t = 0 \qquad (3.44)$$

$$p_{it} = h_i \qquad \forall i \in N,\ t = 0 \qquad (3.45)$$

$$z_{it} = g_i \qquad \forall i \in N,\ t = 0 \qquad (3.46)$$

$$y_{it}^k = f_i^k \qquad \forall i \in N, \forall k \in K,\ t = 0 \qquad (3.47)$$

$$y_{it}^k \in \{0,1\} \qquad \forall i \in N, \forall k \in K, t = 1, \dots, T \qquad (3.48)$$

$$z_{it} \in \{0,1\} \qquad \forall i \in N, t = 1, \dots, T \qquad (3.49)$$

$$p_{it},, s_{it}, r_{it}, w_{it}, \vartheta_{it}, \mu_{it}^{-}, \mu_{it}^{+} \geq 0 \qquad \forall i \in N, t = 1, \dots, T \qquad (3.50)$$

$$q_{it}^{k}, c_{it}^{*k}, b_{it}^{*k}, o_{it}^{k}, n_{it}^{k}, v_{it}^{k}, vv_{it}^{k} \geq 0 \qquad \forall i \in N, \forall\, k \in K, t = 1, \dots, T \qquad (3.51)$$

$$\delta_{t} \geq 0 \qquad t = 1, \dots, T \qquad (3.52)$$

3.3. Illustrative Example

The proposed model is illustrated with several sources of data describing the economy of industries and states and the COVID pandemic characteristics in the United States.

3.3.1. Data

In this study, the data of 50 states, the District of Columbia, and 14 industries are considered. Table 3. 4 shows the definition of the industries and their North American Industry Classification System (NAICS) code, along with their industry-specific rate of COVID-19 infection, the unemployment rate during the pandemic, and the rate of basic inoperability when controlling policy in terms of reduced capacity is applied estimated from the data used in this research are divided into three categories as follows.

1- Economic data

Data for the Input-output model (includes the output of industries in each state (X) and the technical coefficient matrix (A)) are maintained by the Bureau of Economic Analysis (BEA) (2018). Figure 3. 1a shows the gross domestic production (GDP) of each industry in each state as a proxy for the output matrix X. according to this data California, Texas, and New York is the top states with the highest level of GDP. Also, Finance, Government, manufacturing, and professional and business industries are the most productive industries

in these top productive states and the majority of states. Figure 3. 1b also shows that according to the technical coefficient matrix (A), Finance, Manufacturing, and professional and business industries are the neediest industries that need input from the majority of other industries to operate. The technical coefficient is a critical component of inoperability input-output analysis and the controlling policy-making as closing a highly needed industry will propagate to the other industries and fail other industries' operations.

provided by (Chen et al., 2021).

Table 3. 4. The definition and information of the industries considered in this study.

NAIC code	Industry definition	Infection rate (%)	Normalized unemployment rate (%)	Estimated inoperability (%)
11	Agriculture, forestry, fishing, and hunting	9	0	4.6
21	Mining, quarrying, and oil and gas extraction	1	2.9	3.1
22	Utilities	0	0.2	2.3
23	Construction	8	8.9	0.3
31	Manufacturing	9	16.3	2.9
42	Wholesale trade	3	7.5	2.3
45	Retail trade	10	10.5	3.4
48	Transportation and warehousing	5	4.8	4.4
51	Information	1	7.2	1.4
52	Finance, insurance, real estate, rental, and leasing	2	3	0.7
54	Professional and business services	3	22.3	1.5
61	Educational services, health care, and social assistance	4	37.6	3.7
71	Arts, entertainment, recreation, accommodation, and food services	1	100	4.0
92	Government and government enterprises	4	40.2	3.4

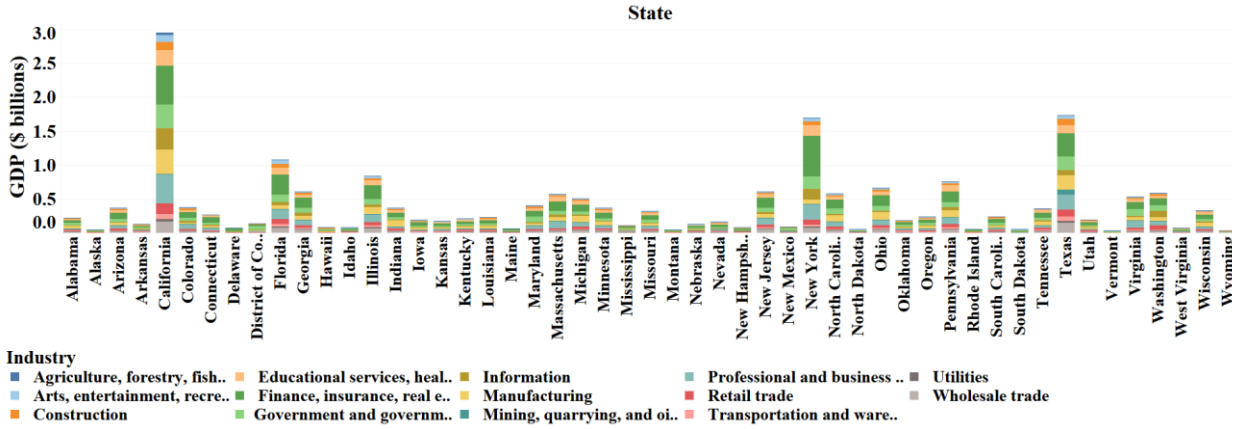

(a)

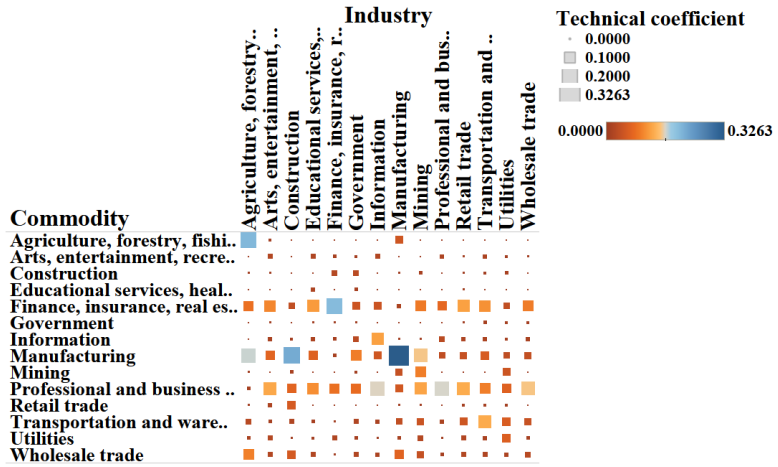

(b)

Figure 3. 1. (a) The output (Gross Domestic Production) of various industries in each state ($ billions) in 2019 (Bureau of Economic Analysis (BEA), 2018), (b) Technical coefficient data (Bureau of Economic Analysis (BEA), 2018).

Data for the commodity flow coefficient (matrix T) are estimated from the Commodity Flow Survey database maintained by the Bureau of Transportation Statistics (BTS) (2017). Figure 3. 2 shows the annual flow of goods in US dollars using multi-modal transportation across different regions in the United States. The majority of the goods flow within each state, therefore in Figure 3. 2, the flow within states is filtered, to depict the significance of between

state flows. Between states, flows are important for developing the pandemic policy as it shows the industry closure in one state will affect other states significantly.

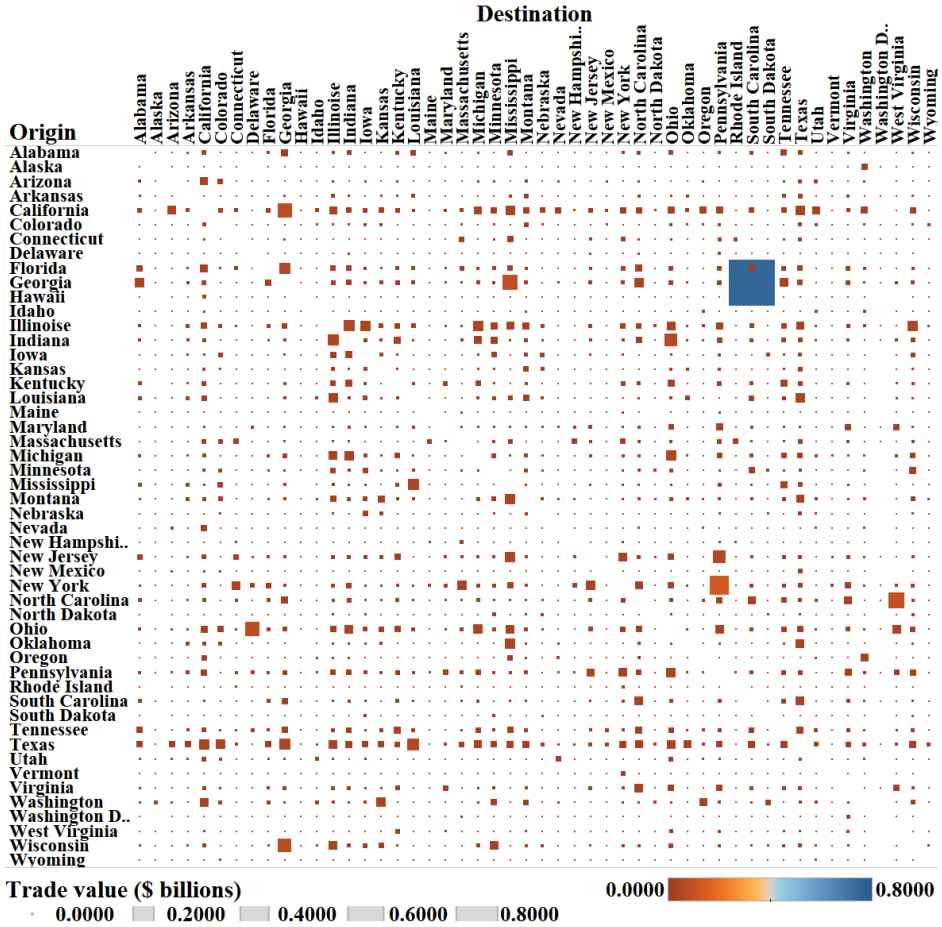

Figure 3. 2. The annual flow of goods using multi-modal transportation across different states ($ billions).

2- Fairness index data

The impact of COVID-19 on individual health and state- and industry-level economic performance differs across states and industries. Therefore, any controlling strategy should consider the social fairness between states and between industries as much as possible. Social fairness is calculated from two components. The first component (ξ_i) measures the risk of getting infected with and dying from COVID-19 in each state(Surgo Ventures, 2021b).

This CCVI index, calculated by (Surgo Ventures, 2021b), incorporates different critical vulnerability factors, such as socioeconomic status, minority, and language status, household and transportation availability, epidemiological factors, healthcare system factors, the riskiness of living and working, and population density. Figure 3. 3 shows the CCVI associated with each state(Surgo Ventures, 2021b).

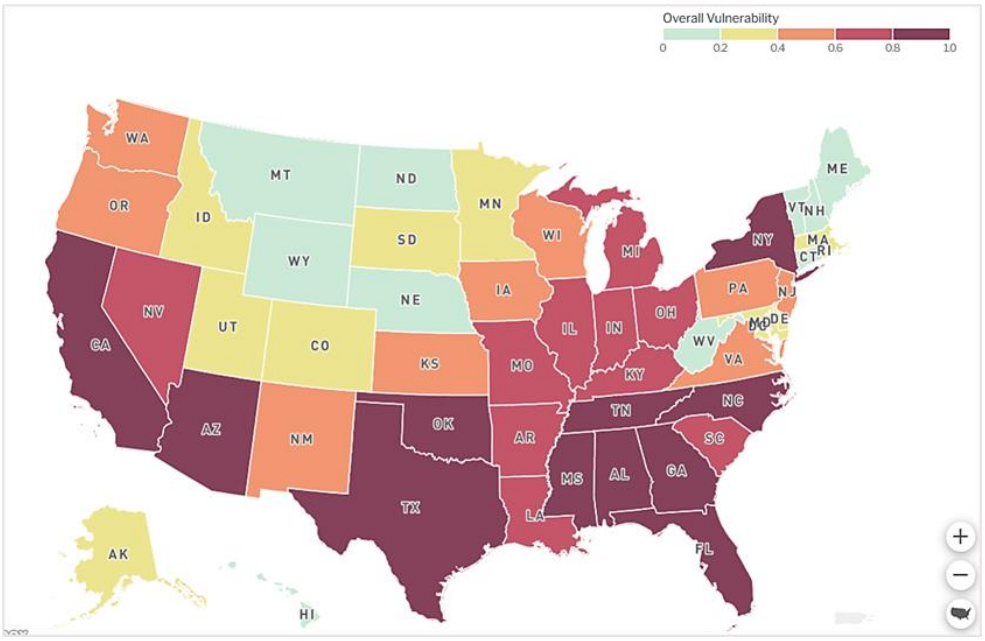

Figure 3. 3. The COVID Community Vulnerability Index (CCVI) across states in the US (Surgo Ventures, 2021b).

The second component of social fairness, (λ_i), measures the vulnerability of employees to lose their job in each state, in terms of the percentage of employees who lost their job due to COVID-19. This value depends on the community attributes of the employees such as age, gender, education level, and race and ethnicity. According to the US Bureau of Labor Statistics (BLS), COVID-19 has changed the employment level in most industries significantly. Figure 3. 4a shows the employment change by industry between February 2020 and February 2021, while Figure 3. 4c shows the distribution of employees over various

industries in each state. Industries such as *Leisure and hospitality*, *Government*, *Educational services*, *Professional and business services*, and *Manufacturing* are the top industries that experienced employee loss due to COVID-19. Also, depending on the combination of employer demography, the vulnerability of losing a job may differ. As is shown in Figure 3. 4b, and according to the US Bureau of Labor Statistics (BLS), women employees, Latino employees, employees with a college education or less, and employees at age of 34-54 have experienced higher rates of unemployment between February 2020 and September 2020. Figure 3. 4d shows the distribution of employees in each state based on different demographic attributes.

To determine the value of λ_i, for each state, we calculated the weighted average over the multiplication of the percentage of job loss in each industry (from Figure 3. 4b) and the percentage of employees in each industry (from Figure 3. 4b) plus the weighted average over the multiplication of the percentage of job loss in each category (from Figure 3. 4c) and the percentage of employee's demography in each industry (from Figure 3. 4d). The normalized value of ξ_i and λ_i for each state is depicted in Figure 3. 5. By using the normalized value of ξ_i and λ_i, Eq.(2.18) measures the total fairness attribute for each state such that if the state is open then the infection vulnerability index should be considered, and if the state is closed the job security vulnerability index should be considered. Then Eq.(2.20) tries to minimize the deviation of the total vulnerability index of each state from the national average vulnerability index to keep fairness among different states.

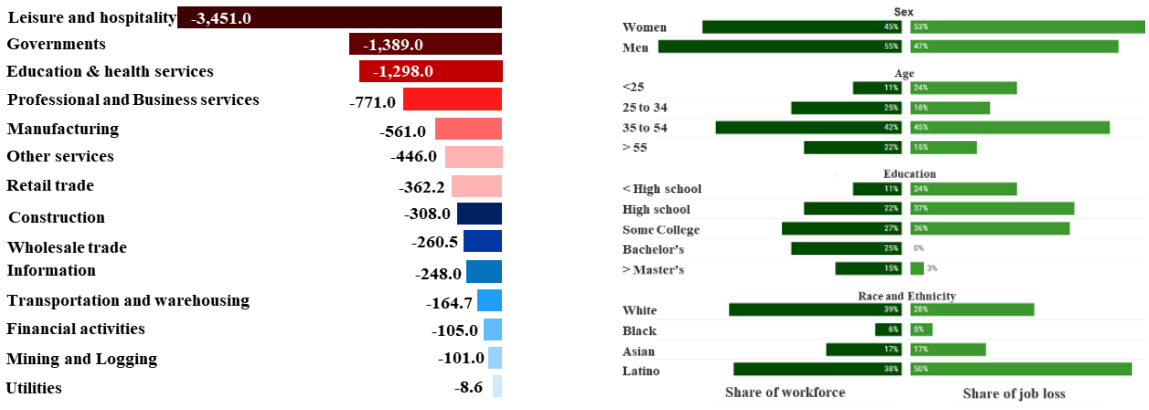

(a) **(b)**

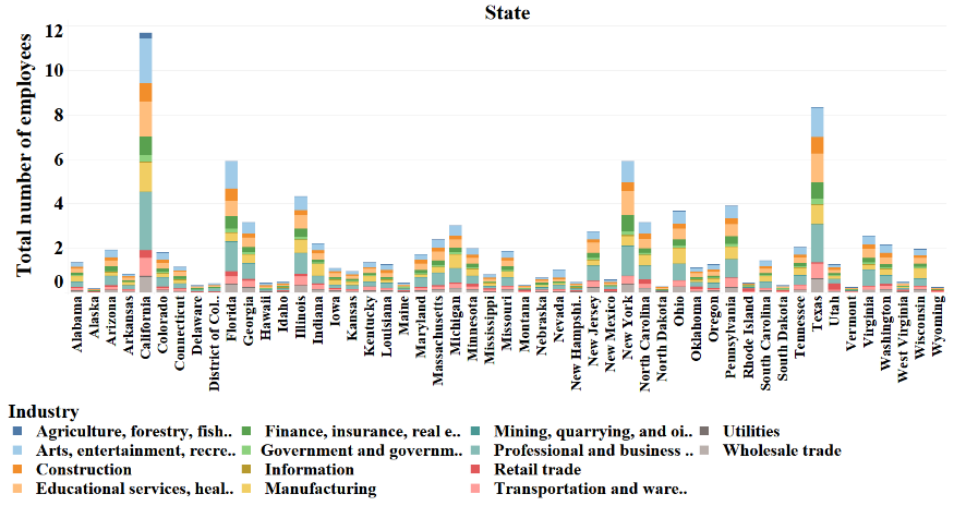

(c)

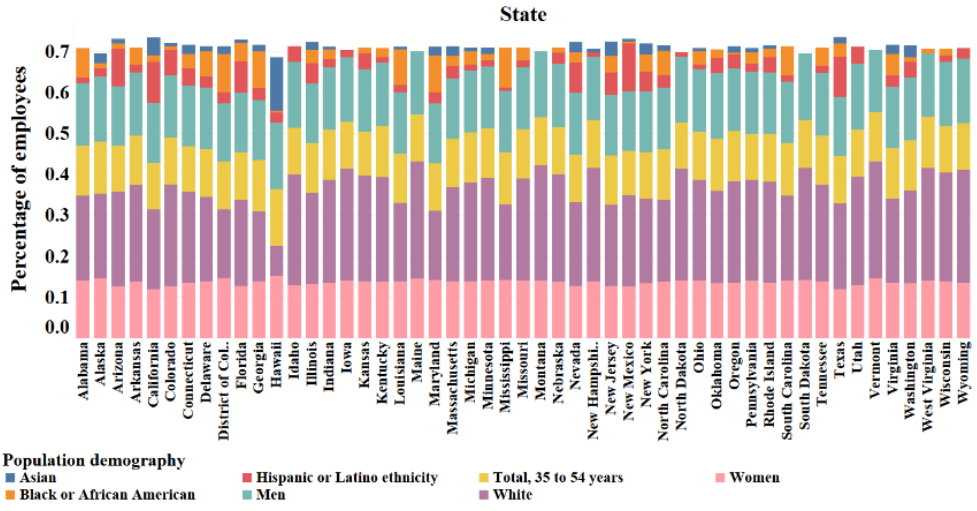

(d)

Figure 3. 4. (a) Employment change by industry (1000), Feb 2020- Feb 2021. (b) The total number of employees of each industry in each state. (c) Share of the workforce as of February 2020 and share of job losses between February 2020-September 2020. (d) demographic distribution of employees in each state.

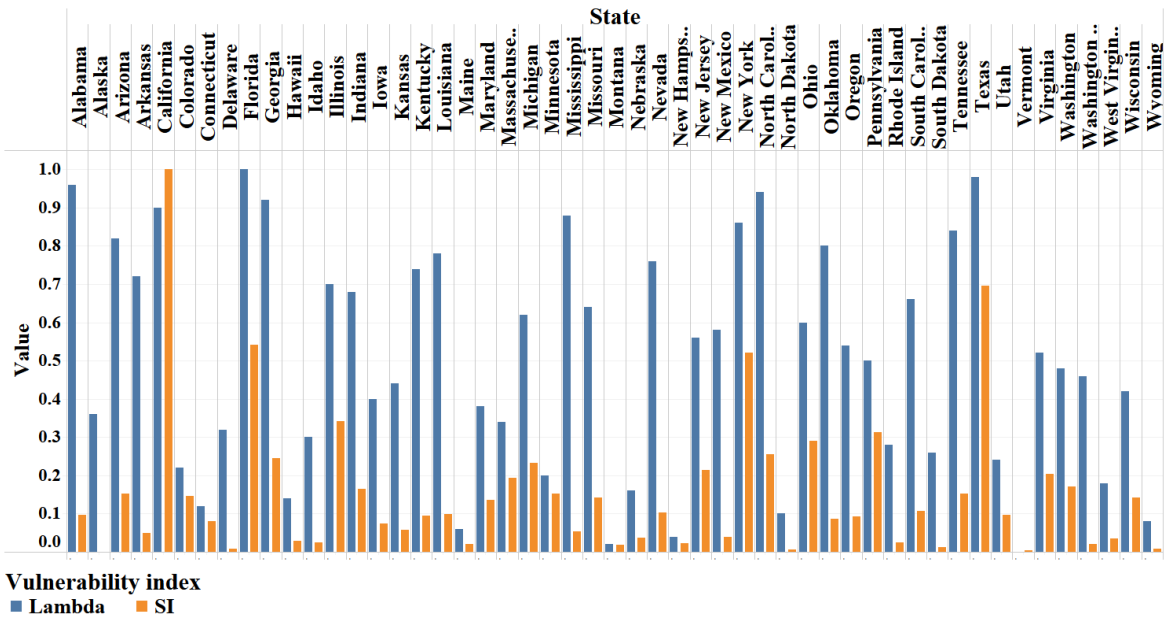

Figure 3. 5. The normalized value of ξ_i and λ_i for each state.

3- COVID-19 data:

These data include the COVID-19-related rates, including the infection, recovery, and death rate at the state level in the United States. These data are gathered from the COVID-19 Impact Analysis Platform compiled by the University of Maryland (University of Maryland, 2020). The average proportion of the total recovery to the total active cases all around the US is equal to 0.6. Data related to the recovery time, death time, and immunity time frame are gathered from the literature and reports from the Centers for Disease Control and Prevention (CDC)[3]. The infection rate in each industry is derived from the Washington state department of health report (Department of Health, 2020). These data show the COVID infection rate in different industries in Washington state, and we have used the same rate for similar industries in all other states.

3 https://www.cdc.gov

According to Kyrychko et al. (2020), the recovery time, t_R vary between 10 to 60. Also, the value of the time to death, t_D, can vary between 0 to 40 days. The time interval in our analysis is considered equivalent to 14 days. Therefore, we assume that $t_R = 4$ (equivalent to 28 days) and $t_D = 1$(equivalent to 14 days). According to the CDC, evidence suggests that reinfection is uncommon three months after the initial infection. Therefore, we consider the immunity time $t_V = 6$ in the model. At the initial time $t = 0$, all industries, and states are considered open.

3.3.2. Solution Approach

We utilize the augmented ε-constraint method proposed by (Mavrotas & Florios, 2013) to solve the proposed multi-objective MOMILP model. The augmented ε-constraint method (AUGMECON) is an efficient version of the ε-constraint method, which accelerates the process of generating Pareto-optimal solutions by avoiding redundant iterations.

All the implementations in this study are performed on a 64-bit desktop system with 12.0 GB RAM and the Core-i7-6500U CPU@2.5GHz. The proposed framework is modeled and solved by Gurobi in Python and the implementation of each AUGMECON run takes 1 to 6 hours with at least a 5-10% optimality gap.

3.4. Results

To generate the Pareto optimum solutions, we consider 5×5 grid points and the results for the normalized payoff matrix and range of three objective functions are shown in Table 3. 5. The Pareto optimum solution is also shown in Figure 3. 6. The epidemiologic and economic impacts are negatively correlated through the industry status variable (y_{it}^k), the

epidemiologic and social impacts are affecting each other through the state status variable (x_{it}) and there is no correlation between economic impact and the social impact. When looking for the optimum policy for controlling all three impacts of the pandemic, the model tries to decrease the economic impact by keeping more industries. However, since opening states and all industries would significantly increase the number of patients, the model chooses to close states with less social impact and less demanded industries.

Table 3. 5. The normalized payoff matrix and range of three objective functions.

	$F1$ value	$F2$ value	$F3$ value
Min $F1$	0	1	1
Min $F2$	0.556	0	0.458
Min $F3$	1	0.721	0

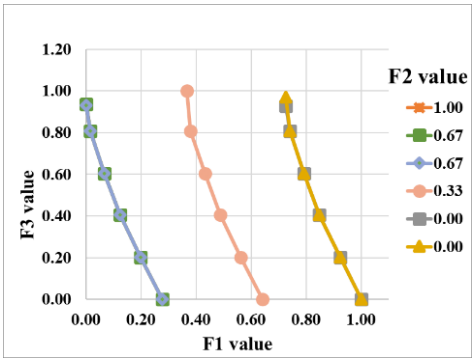

Figure 3. 6. The Pareto-optimal solutions for the proposed MOMILP.

Figure 3. 7 shows the change in normalized values of the three impacts when the proposed model is solved for the different single objective functions and a multi-objective over the time horizon of 14 weeks ($T = 7$). For the sake of compression of the four objective functions, we choose a solution from the Pareto-optimal set that results in the minimum cubic distance from the lower bound of each objective in that specific scenario. For instance, among the 25 Pareto-optimal solutions, one of the solution points has the lowest cubic distance from the minimum values of F1, F2, and F3 from the payoff matrix. The selected Pareto-optimal solution results in the normalized values of the three objective functions such that F1= 0.56, F2=0.89, and F3=0.66.

If the epidemiological impact is the only focus of policymakers, $min\ F1$ would result in the smallest infected population over the first two periods. This causes several states and industries to close, which increases inoperability significantly. Also, when the states are closed, under-presented communities may lose other jobs. If the policymaker's focus is on maintaining fair decisions with respect to demographic and COVID vulnerability ($min\ F2$), then the number of patients and the inoperability of industries would increase as states and industries may close and reopen frequently. The proposed MOMILP results in significantly different outcomes such that the optimal values of each objective are roughly close to each other, while in the first three scenarios, the range of each objective is significantly higher. The derived strategy would result in higher epidemiologic impact, lower social impact, and lower inoperability compared to when the focus is placed on decreasing epidemiologic impact. It also results in higher social and higher inoperability compared to when all focus is on the social impact. The results from all three MOMILP objective functions are more convincing for policymakers interested in minimizing all three aspects of the pandemic impact. The selected Pareto solution suggests closing more states and more industries. However, this results in a higher unbalanced solution for the social impact, and it creates more economic issues stemming from the increase in the lost jobs.

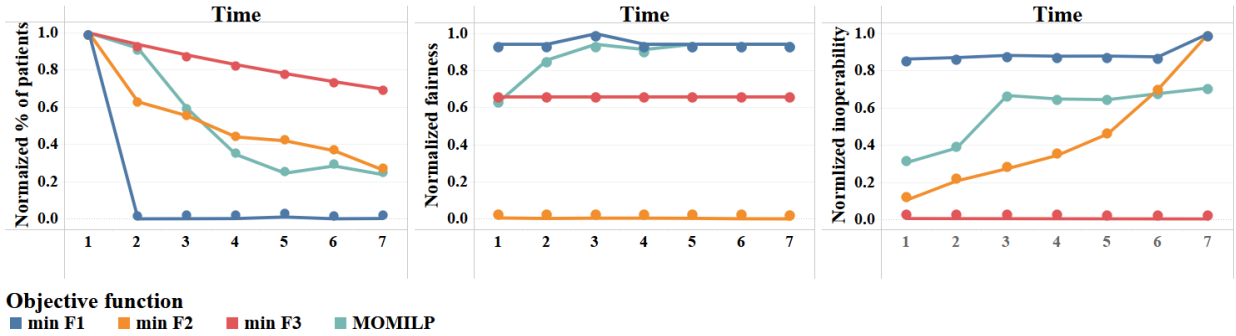

(a) **(b)** **(c)**

Figure 3. 7. The results of the proposed model for (a) Normalized average percentage of patients, (b) Normalized average social impact, and (c) Normalized average inoperability.

Every Pareto-optimal solution provides the timing of required changes in the state and industry status. Figure 3. 8 shows the optimal opening and closure policy for each state and industry over the time horizon for the selected solution. At the beginning of the planning horizon, all states and industries are open. Due to the increase in the number of infections, the model starts with closing the states with high populations such as Illinois, Texas, and California among others. It also closes industries with a lower impact on the inoperability while having a higher number of employees, such as state and industries get closed and after the decline in the number of patients, the model opens states and industries selectively so it does not cause high social and inoperability impacts.

Figure 3. 8 shows the state and the industry status over the time horizon derived from the selected Pareto-optimal solution. The interregional technical coefficient plays an important role in defining the industry status. The model tries to keep the critical industries open more often. These industries whose closure results in high inoperability (Chen et al., 2021) include *Professional and business services*, *Finance*, *Manufacturing*, and *Government*. According to Figure 3. 1b, the need of other industries for the commodity of these three

industries is also high. Among the industries whose interregional technical coefficient is low, *Construction*, *Educational services*, and *Mining* are closed more often.

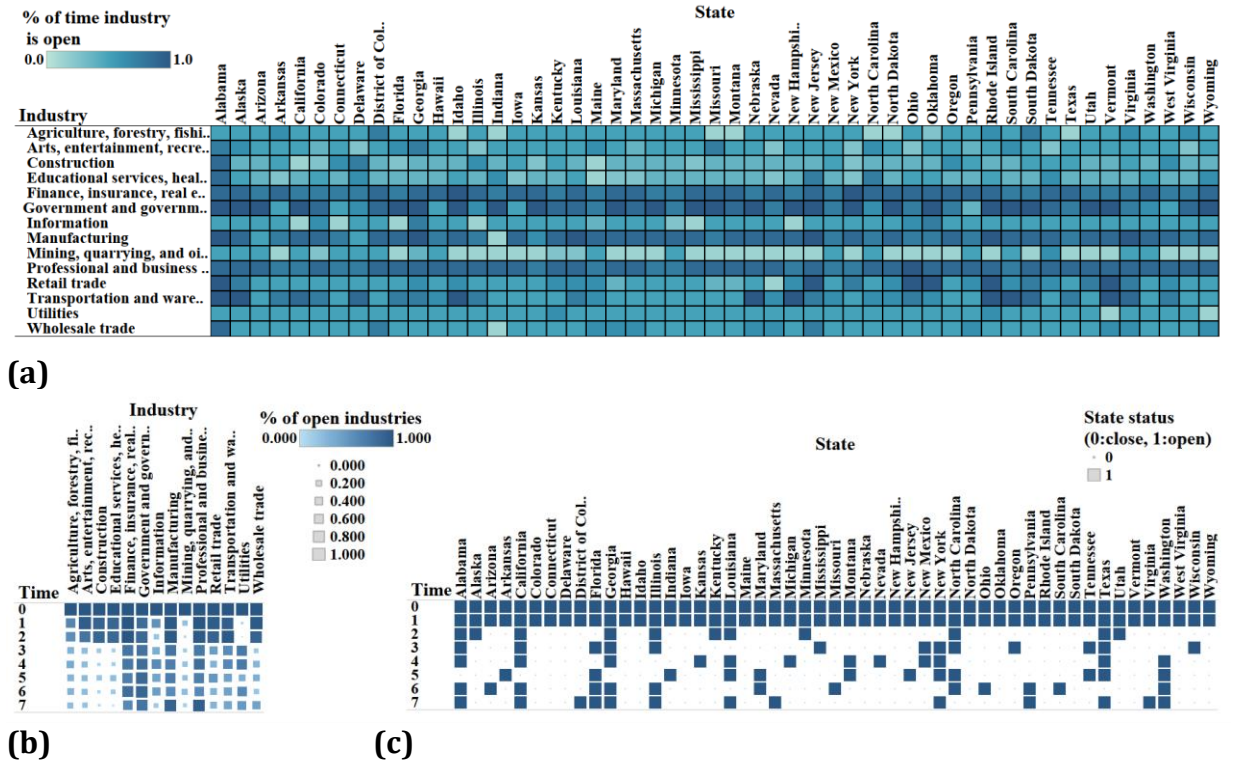

Figure 3. 8. State and industry level policy for the selected Pareto optimum solution. (a) the percentage of time that each industry in each state is open, (b) the percentage of open industries over the planning time horizon, and (c) the state status over the planning time horizon.

The results show that Alabama, California, Florida, Georgia, Illinois, Louisiana, New York, North Carolina, Texas, and Washington are the states that should open more often. Although the high population of these states causes a high rate of infection, the demographic attribute of the population, the COVID vulnerability index, and the scale of employees and their job security index in this state play a critical role in determining the state's status. Therefore, the model keeps these states open so that the social vulnerability attribute is as close as possible to the national average

Figure 3. 9. shows the value of the three target impacts of the selected policy at the state and industry levels over the planning horizon. According to Figure 3. 9a at time 0, all states and industries are open, resulting in an epidemiological impact at time 1. The first two periods show a high percentage of infections as more industries and states are open, then the model starts closing states and industries. California, Georgia, North Carolina, and Alabama experience a high rate of infections as they are more open under the selected policy. Figure 3. 9b shows the social vulnerability index resulting from the selected policy. States whose closure causes a high deviation from the national social vulnerability index are forced to stay open more often by the proposed model. California, Florida, Illinois, New York, North Carolina, Ohio, Pennsylvania, and Texas experience fewer unfair decisions under the selected policy. This is compatible with the fact that these are large states with the highest variation in the demographic index and also a higher COVID vulnerability index. Therefore, the model tries to give more weight to the social vulnerability index, in order to keep the social impact minimum and to keep the fairness between states higher. Colorado, Connecticut, Delaware, Idaho, Iowa, Minnesota, Nebraska, Utah, and West Virginia are states where the social vulnerability index is high, and they are experiencing higher adverse social impact. Figure 3. 9c shows the inoperability caused by the selected policy. *Agriculture*, *Mining*, *Utility*, *Construction*, *Education*, *Finance*, *Art*, and *Government* industries have the highest levels of interstate trade and the least amount of intrastate trade, suggesting that the closure of these industries causes high interstate inoperability. More specifically, the closure of industries such as *Manufacturing*, *Professional businesses*, *Transportation*, and *Wholesale*, especially in states such as California, Louisiana, Texas, Washington, and Georgia, will result in high interstate inoperability.

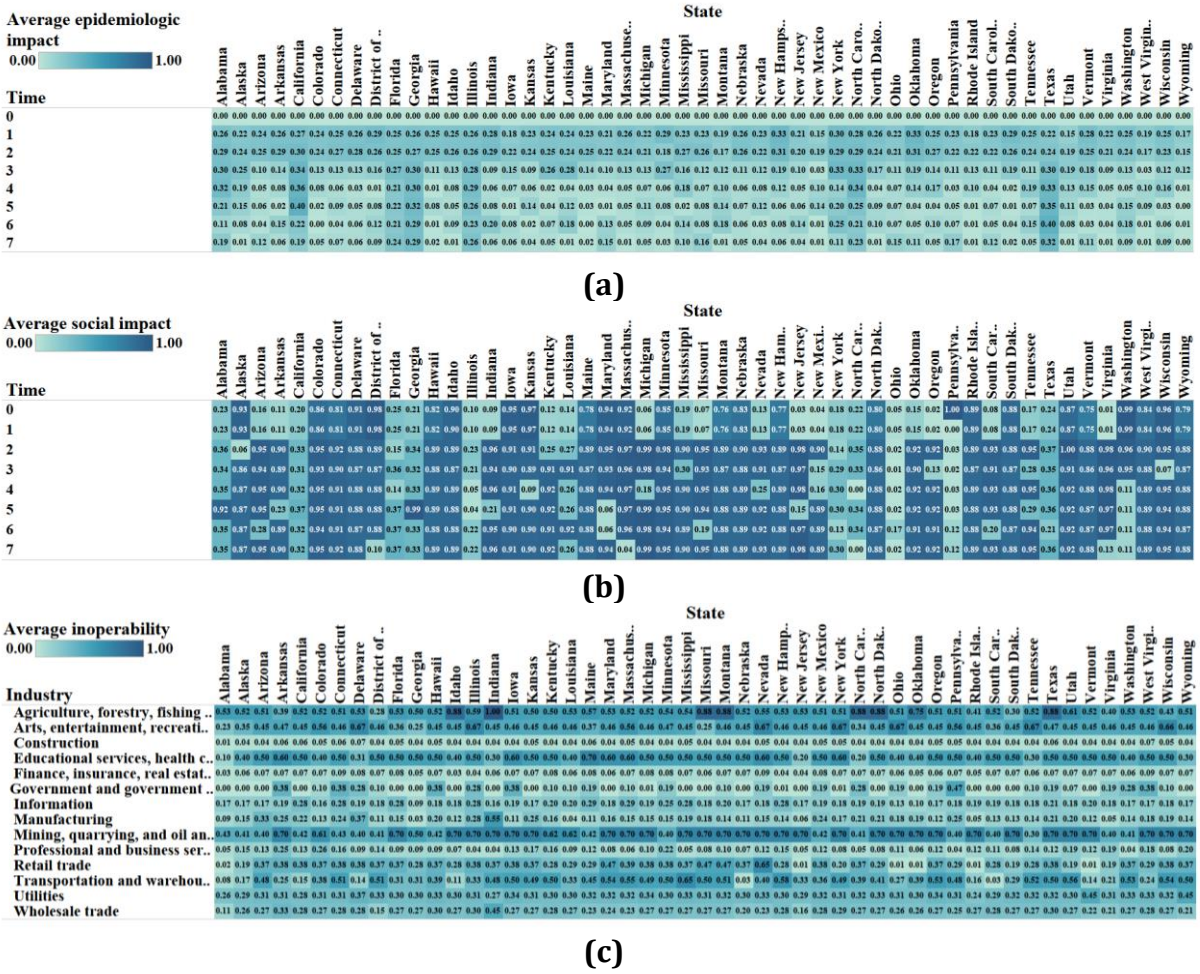

Figure 3. 9. State and industry level policy for the selected Pareto optimum solution. (a) the normalized average percentage of patients in each state over the planning time horizon, (b) the normalized average of the social vulnerability index in each state over the planning time horizon, and (c) the normalized average inoperability of each industry over the planning time horizon.

To explain the importance of considering the social and the economic impact of a pandemic along with the epidemiologic impact, we selected two states randomly (here California and Pennsylvania) and analyzed the results based on the industries' status shown in Figure 3. 10, the inter-regional and inter-industrial dependencies based on the technical coefficients shown in Figure 3. 1b and the normalized trade flow information shown in Figure 3. 11 and Figure 3. 12.

3.4.1. Analysis of Inoperability in California

According to the commodity flow survey, 50% and 52% of commodity trade flow within California and Pennsylvania, respectively. The top state recipients of commodities exported from California are Nevada, Arizona, and Hawaii, mainly from industries such as *Retail trade*, Transportation and warehousing, and *Professional and business services*. So, any inoperability in these industries will result in subsequent inoperability in the destination state's industries. On the other hand, California imports mostly from Arizona, Utah, and Colorado, and from industries such as *Mining*, *Transportation and warehousing*, and *Information*. So, if any of these industries experience failure, interdependent industries in California will experience some level of inoperability. Figure 3. 9 shows that the highest inoperability of industries in California belong to *Agriculture*, *Education*, *Arts*, *Mining*, *Retail trade*, *Wholesale trade*, *Information*, and *Utilities*. The inoperability of *Agriculture*, *Education*, and *Arts* stem from the closure of these industries in California after times $t = \{1,4\}$ and $t = 3$ respectively. The *Mining* industry requires commodities mostly from *Manufacturing*, *Professional and business services*, *Finance*, and *Mining* industries. Almost 80% of these commodities are supplied from California, Utah, Arizona, and Montana. The closure of *Mining* in-between time $t = 1$ and $t = 7$ in Utah and Montana, and at time $t = \{3,4\}$ and time $t = \{6,7\}$ in California, cause the main inoperability in the *Mining* industry in California. Closure of *Manufacturing* at time $t = 5$ and $t = 6$ in California and Utah, respectively, the closure of *Professional and business services* at times $t = 3, t = \{6,7\}$ in California and Arizona, respectively, and the closure of *Finance* at times $t = \{6,7\}$ in California are the other sources of the inoperability in *Mining*. Similarly, the inoperability of *Retail trade* requires more than 50% of its input from *Professional and business services*, *Finance*, *Transportation*,

Manufacturing, *Utilities*, *Wholesale*, and *Information*. The inoperability of *Retail trade* in California stems from the closure of *Professional and business services* at times $t = 3$ and $t = \{6,7\}$ in California and Arizona, respectively, and the closure of *Finance*, *Utilities*, and *Information*, respectively, at times $t = \{6,7\}$, $t = \{1,2,5,6\}$, and $t = \{1,2,3,4,5,6,7\}$ in California. The inoperability of *Retail trade* also stems from the closure of *Transportation* in California and Mississippi at the time $t = \{7\}$ and $t = \{1,5,6,7\}$, respectively, and the closure of *Manufacturing* in California and Georgia at times $t = \{5\}$ and $t = \{6\}$ respectively and the closure of *Wholesale trade* in California, Texas, and Michigan at times $t = \{3,4,5,6,7\}$, $t = \{3, 5,6,7\}$ and $t = \{3,4,6,7\}$, respectively. Similar analysis can be done for the *Wholesale trade*, *Information*, *Utilities*, and other industries in California using the commodity flow information, technical coefficient table, and the optimal pandemic policy.

3.4.2. Analysis of Inoperability in Pennsylvania

Pennsylvania imports mostly from West Virginia, New Jersey, New York, Ohio, and Virginia from industries such as Mining, *Professional and business services*, and *Wholesale trade*. The top state recipients of exports from Pennsylvania are Delaware, New Jersey, and Maryland, mainly from industries such as *Professional and business services*, *Transportation and warehousing*, *Information*, and *Manufacturing*. Therefore, any failure in these industries in Pennsylvania will cause some levels of inoperability in the other industries in interdependent states. For example, according to Figure 3. 1b the commodity of the *Professional and business services* industry is mainly required by itself and *Information*, *Retail* and *Wholesale trade* industries. *Professional and business services* are only closed at time $t = 6$, therefore it contributes the most to the inoperability of the four independent industries in

Wyoming, Connecticut, Pennsylvania, Ohio, and DC. The commodity of *Transportation* industry is mainly required by itself and *Utilities*, and *Retail trade* industries. *Transportation* industry in Pennsylvania is closed at time $t = \{3,4,6,7\}$ and this closure mainly contributes to the inoperability of the *Transportation Utilities*, and Retail trade industries in Pennsylvania, Delaware, and Maryland. The effect of the pandemic policy on the propagation of the inoperability to different industries in different states can be analyzed similarly.

3.4.3. Social impact

The proposed model decides about the state status based on the epidemiologic impact (number of infected populations in each state influenced by the specific infection rate and the population of the state) and the social effect (deviation from the national social vulnerability level at each time). The decision of state status is part of a national decision, and the status of every state depends on the status of the other state so that the epidemiologic impact and the social impact at the national level are minimized. In combination with the status of other states, the model decides to open California more often than Pennsylvania. In general, the epidemiologic impact is more significant than the social impact in the model and the model opens. According to Figure 3. 5, California has the highest CCVI value ($\xi_i = 1$) in the United States. This means if California stays open for a longer time, the percentage of the infected population goes up significantly. However, California has also a high ratio of vulnerable communities losing their job ($\lambda_i = 0.9$) if the state got closed more often. In comparison, Pennsylvania has a moderate CCVI value ($\xi_i = 0.5$) and ratio of vulnerable communities to losing their job ($\lambda_i = 0.3$). So closing and opening Pennsylvania would result in a moderate social impact while the status of California is critical.

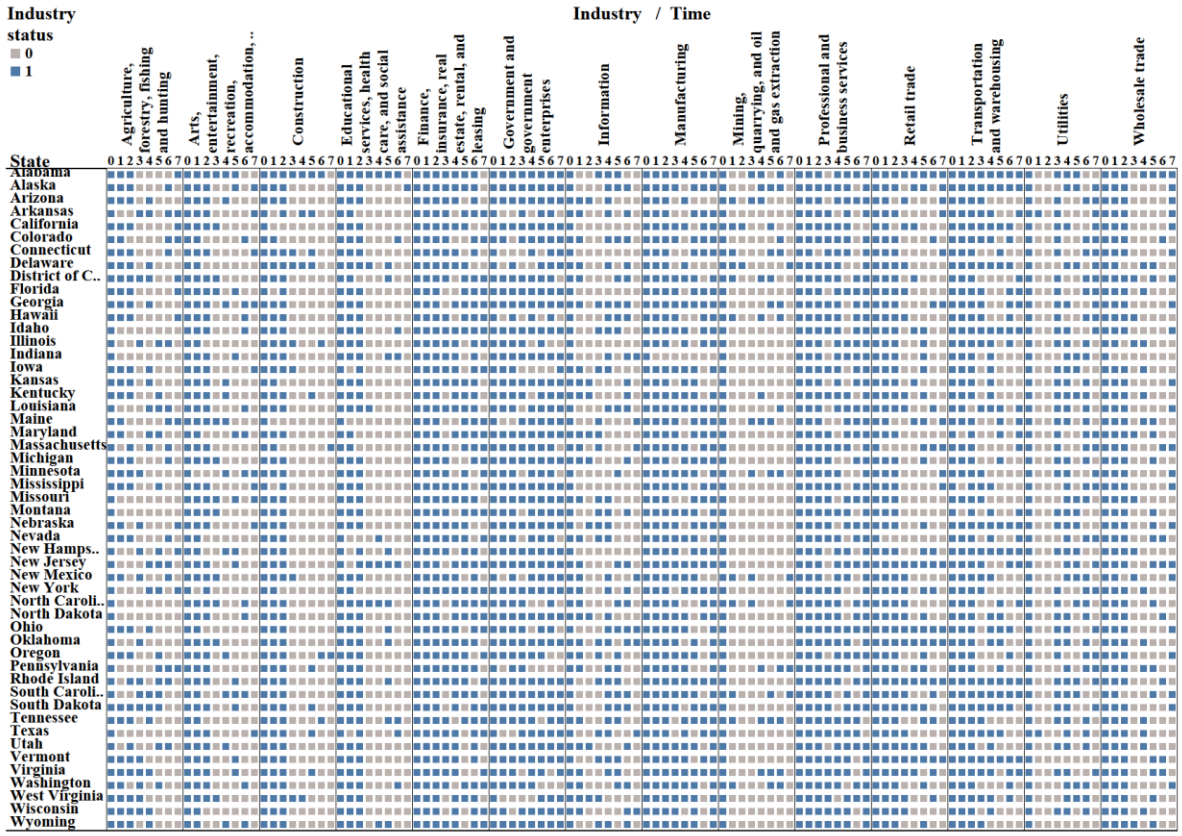

Figure 3. 10. The status of industries in each state over the planning horizon from the selected Pareto optimum solution.

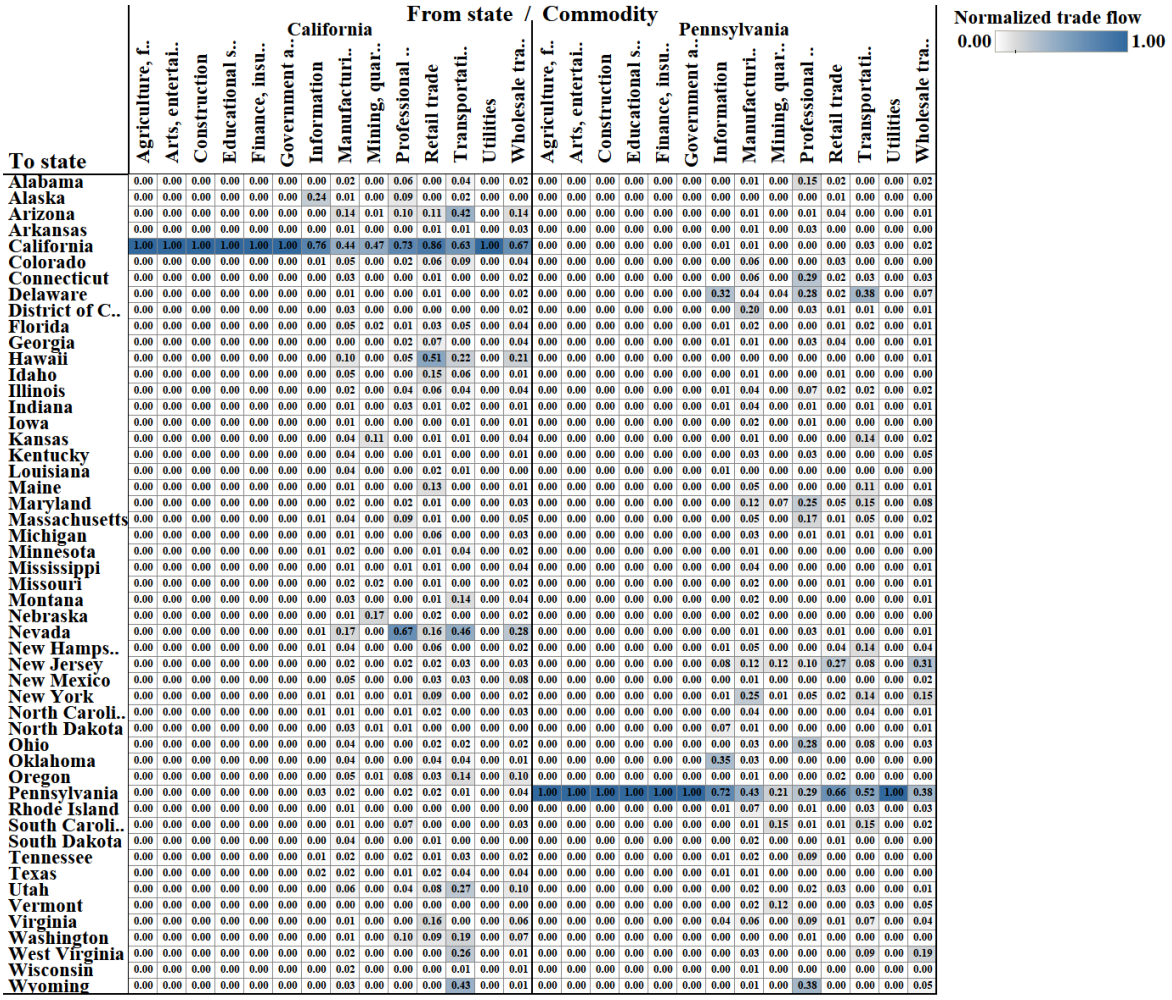

Figure 3. 11. The normalized flow of commodities from California and Pennsylvania to different states.

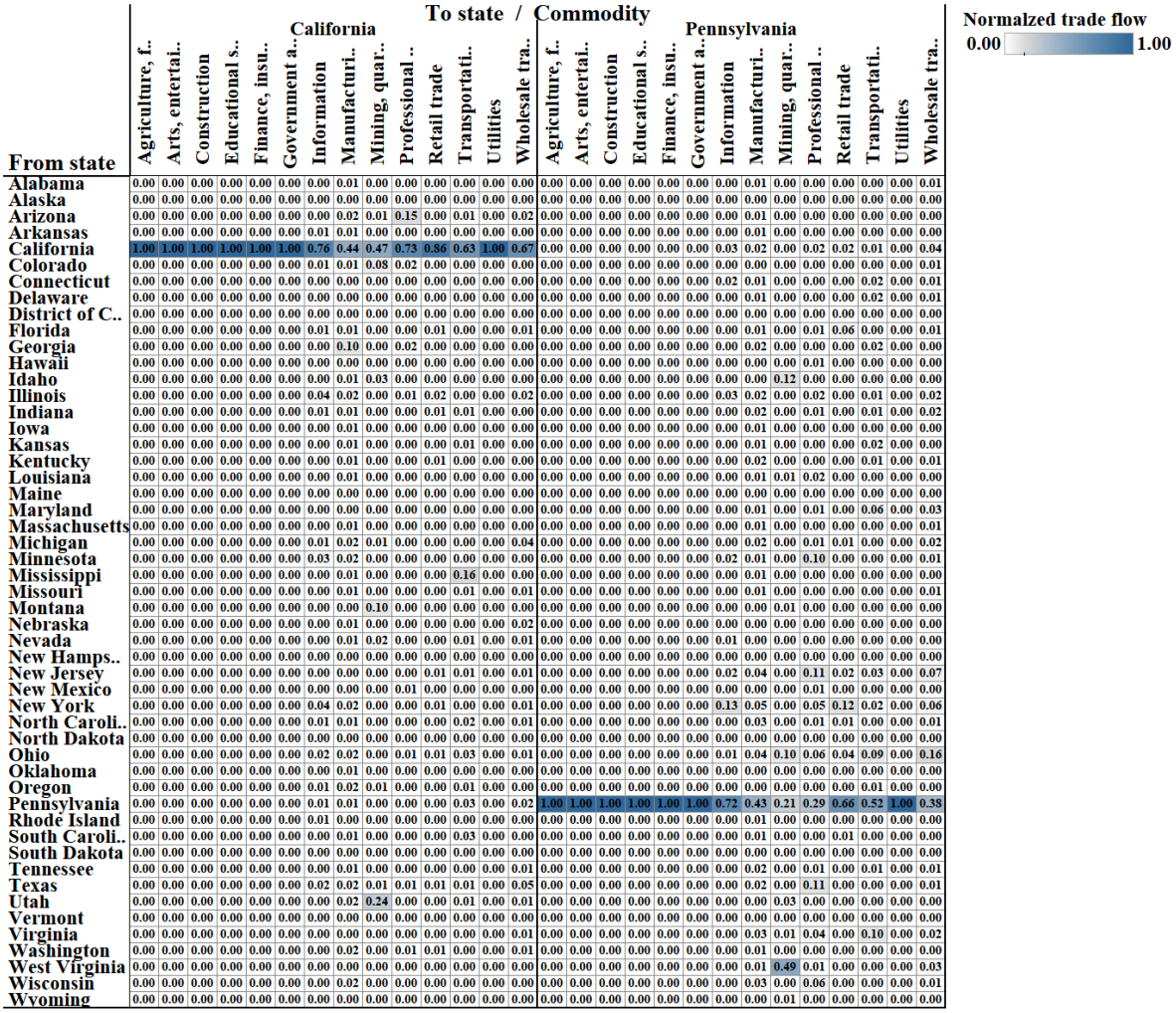

Figure 3. 12. The normalized flow of commodities from different states to California and Pennsylvania.

3.5. Concluding remarks

This research explores a improve state-level and industry-level operational decisions during pandemic outbreaks while minimizing three critical impacts of the pandemic including the epidemiologic impact, the social impact of the decisions for each state, and the inoperability caused by the industry-level decisions. The proposed model integrates SIRD and MRIIM models into a mixed-integer linear programming model for estimating the best-control strategy during a pandemic over a specified time horizon. The contribution of this

paper lies in (i) proposing a prescriptive decision-making tool, based on a multi-objective mixed-integer linear programming optimization model which results in an optimum policy to control pandemics at the state and industry level, and (ii) proposing a decision-making model that incorporates the societal fairness, the epidemiologic impact, and the inoperability impact of the pandemic in deriving the optimum controlling policy, (iii) considering the social attribute from two aspects including the vulnerability of social communities to both getting infected by COVID due to the open state and losing a job due to the state closure, measured by the deviation from the national social vulnerability index, and (iv) quantifying the inoperability impact of a pandemic by combining the supply side multi-regional inoperability model (MRIIM) and the industry level decisions within the optimization model.

The proposed framework minimizes three main components: (i) the epidemiological impact measured by SIRD formulation, (ii) the deviation of the social vulnerability index in each state from the national average social vulnerability index, and (iii) the economic impact measured by the inoperability of industries caused by industry closure. While the state and industry closure result in lower epidemiologic impact, the industry closure increases the industry's inoperability. Also, the state reopening contributes to the number of infected populations, which ultimately impacts the workforce effectiveness of the industries, closing states contributes to the job losses in different social communities and industries, and finally, it impacts the economy of the states un-equally. Therefore, the timing and the choice of closure and reopening of states and industries are important for minimizing the epidemiologic, social, and economic impact of the pandemic.

The proposed model is implemented on the COVID-19 data from over 50 states, the District of Columbia, and 14 industries in the US. The results show that with a different combination of epidemiologic, social, and economic components, some states have shown a high percentage of patients in some scenarios while others have shown a high level of job losses. Furthermore, the closure of each industry in one state may affect another industry's output in the same or other states and therefore affect the closure or opening of industries in the same or other states. Therefore, the proposed multi-objective mixed-integer linear programming tries to find a balanced control policy for each state and industry and at each period to diminish all three impacts of the pandemic simultaneously.

As such, future work will explore (i) incorporating various levels of the strictness of the control policy based on the criticality of industries, businesses, and states, and (ii) measuring the effect of the adoption and the timing of vaccination on the optimal closure and reopening strategies, and (iii) examining the efficacy of the decision-making level, by comparing national, regional and state level aspects of socio-economic fairness.

Chapter 4: Concluding Remarks

4.1. Summary and Conclusions

The core of this thesis is to design a decision-making tool to evaluate the impact of the pandemic on the social, economic, and health of the countries and optimize the policy which can minimize all three adverse impacts of the pandemic. For this purpose, we combined required models which measure each aspect of the pandemic crisis: the SIRD model for measuring the epidemiologic impact, MNFP for the economic impact on the interstate trade and the unmet demand of the final consumers, the MRIIM model to quantify the inoperability of industries due to their dependencies to the output of other industries in same or other states, and the vulnerability of social communities in each state against pandemic health and economic threats. The proposed framework involves two main decisions: (i) when each state should be closed and when it should reopen and (ii) when each industry in each state should be closed and when it should reopen. We establish three objectives to address all three aspects of pandemic impact and this motivates the need for using appropriate algorithms such as variations of epsilon constraint methods. Therefore, we use the Augmented epsilon constraint method which tries to optimize one of the objectives and push the other two objectives toward their optimum values by setting lower bounds on the two objectives in a combination of intervals.

The results of the first model show that with a different combination of economic and epidemiologic components, some states have shown a high percentage of patients in some scenarios while others have shown a high level of negative economic impact. Furthermore, the closure of each industry in one state may affect the unmet demand in another state and

therefore affect the closure or opening of industries in the same or other states. Therefore, the proposed multi-objective mixed-integer linear programming tries to find a balanced control policy for each state and industry and each time to diminish the economic and epidemiological impact of the pandemic simultaneously.

The results of the second model show that with a different combination of epidemiologic, social, and economic components, some states have shown a high percentage of patients in some scenarios while others have shown a high level of job losses. Furthermore, the closure of each industry in one state may affect another industry's output in the same or other states and therefore affect the closure or opening of industries in the same or other states. Therefore, the proposed multi-objective mixed-integer linear programming tries to find a balanced control policy for each state and industry and at each period to diminish all three impacts of the pandemic simultaneously.

4.2. Future Directions

Analyzing the impact of the pandemic on the socio-economic systems is not an easy task. The inherent complexities, nonlinear functional interdependencies, stochastic behavior, and temporal uncertainties of cyber-physical-social systems have made them significantly vulnerable to failure, causing substantial risks to national, social, and economic security. Different details can be added to the proposed model which makes it more applicable to the real-world situation. Future work will explore (i) incorporating various levels of the strictness of the control policy based on the criticality of industries, businesses, and states, and (iii) measuring the effect of the adoption and the timing of vaccination on the optimal closure and reopening strategies.

References

Abiad, A., Arao, R. M., & Dagli, S. (2020). The economic impact of the COVID-19 outbreak on developing Asia.

Ahmad, T., Haroon, M. B., & Hui, J. (2020). Coronavirus Disease 2019 (COVID-19) Pandemic and economic impact. *Pakistan journal of medical sciences, 36*(COVID19-S4), S73.

Andersen, T. M., Schröder, P. J., & Svarer, M. (2020). *Designing Reopening Strategies in the Aftermath of COVID-19 Lockdowns: Some Principles with an Application to Denmark*: IZA-Institute of Labor Economics.

Aspri, A., Beretta, E., Gandolfi, A., & Wasmer, E. (2021). Mortality containment vs. economics opening: optimal policies in a SEIARD model. *Journal of mathematical economics, 93*, 102490.

Atkeson, A., Droste, M. C., Mina, M., & Stock, J. H. (2020). *Economic benefits of covid-19 screening tests*. Retrieved from

Baldwin, R., & Tomiura, E. (2020). Thinking ahead about the trade impact of COVID-19. *Economics in the Time of COVID-19, 59*.

Balla-Elliott, D., Cullen, Z. B., Glaeser, E. L., Luca, M., & Stanton, C. T. (2020). *Business reopening decisions and demand forecasts during the COVID-19 pandemic* (0898-2937). Retrieved from

Barua, S. (2020). Understanding Coronanomics: The economic implications of the coronavirus (COVID-19) pandemic.

Bauer, L., Broady, K., Edelberg, W., & O'Donnell, J. (2020). Ten facts about COVID-19 and the US economy. *Brookings Institution, 17*.

Bertsimas, D., Boussioux, L., Cory-Wright, R., Delarue, A., Digalakis, V., Jacquillat, A., . . . Mingardi, L. (2021). From predictions to prescriptions: A data-driven response to COVID-19. *Health care management science*, 1-20.

Blustein, D. L., Duffy, R., Ferreira, J. A., Cohen-Scali, V., Cinamon, R. G., & Allan, B. A. (2020). Unemployment in the time of COVID-19: A research agenda. In: Elsevier.

Blustein, D. L., & Guarino, P. A. (2020). Work and unemployment in the time of COVID-19: the existential experience of loss and fear. *Journal of Humanistic Psychology, 60*(5), 702-709.

Bonet-Morón, J., Ricciulli-Marín, D., Pérez-Valbuena, G. J., Galvis-Aponte, L. A., Haddad, E. A., Araújo, I. F., & Perobelli, F. S. (2020). Regional economic impact of COVID-19 in Colombia: An input–output approach. *Regional Science Policy & Practice, 12*(6), 1123-1150.

Brodeur, A., Gray, D. M., Islam, A., & Bhuiyan, S. (2020). A Literature Review of the Economics of COVID-19.

Bureau of Economic Analysis (BEA). (2018). Interactive Access to Input–Output Accounts Data. Retrieved from http://www.bea.gov.in. Retrieved 2022 http://www.bea.gov.in

Bureau of Labor Statistics. (2022). *THE EMPLOYMENT SITUATION —MAY 2022*. Retrieved from https://www.bls.gov/cps/effects-of-the-coronavirus-covid-19-pandemic.htm

Bureau of Transportation Statistics. (2020). Transportation-Commodity Flow Survey: United States: 2017. Retrieved from https://www.bts.gov/cfs. https://www.bts.gov/cfs

Bureau of Transportation Statistics (BTS). (2017). 2017 Commodity Flow Survey Overview and Methodology, . Retrieved from <http://www.bts.gov/publications/commodity_flow_survey. Retrieved 2022 <http://www.bts.gov/publications/commodity_flow_survey

Buso, I. M., De Caprariis, S., Di Cagno, D., Ferrari, L., Larocca, V., Marazzi, F., . . . Spadoni, L. (2020). The effects of COVID-19 lockdown on fairness and cooperation: Evidence from a lablike experiment. *Economics letters, 196*, 109577.

Cariappa, A. A., Acharya, K. K., Adhav, C. A., Sendhil, R., & Ramasundaram, P. (2021). COVID-19 induced lockdown effects on agricultural commodity prices and consumer behaviour in India–Implications for food loss and waste management. *Socio-Economic Planning Sciences*, 101160.

Chen, J., Vullikanti, A., Santos, J., Venkatramanan, S., Hoops, S., Mortveit, H., . . . Marathe, M. (2021). Epidemiological and Economic Impact of COVID-19 in the US. *Scientific reports, 11*(1), 1-12.

Chetty, R., Friedman, J., Hendren, N., & Stepner, M. (2020). The economic impacts of COVID-19: Evidence from a new public database built from private sector data. *Opportunity Insights*.

Choi, W., & Shim, E. (2021). Optimal strategies for social distancing and testing to control COVID-19. *Journal of theoretical biology, 512*, 110568.

Chowell, G., & Mizumoto, K. (2020). The COVID-19 pandemic in the USA: what might we expect? *The Lancet, 395*(10230), 1093-1094.

Cohen, G. D. (2020). Measuring employment during COVID-19: Challenges and opportunities. *Business Economics, 55*(4), 229-239.

Cowger, T. L., Davis, B. A., Etkins, O. S., Makofane, K., Lawrence, J. A., Bassett, M. T., & Krieger, N. (2020). Comparison of weighted and unweighted population data to assess inequities in coronavirus disease 2019 deaths by race/ethnicity reported by the US Centers for Disease Control and Prevention. *JAMA network open, 3*(7), e2016933-e2016933.

Crowther, K. G., & Haimes, Y. Y. (2010). Development of the multiregional inoperability input-output model (MRIIM) for spatial explicitness in preparedness of interdependent regions. *Systems Engineering, 13*(1), 28-46.

Das, I., & Dennis, J. E. (1998). Normal-boundary intersection: A new method for generating the Pareto surface in nonlinear multicriteria optimization problems. *SIAM journal on optimization, 8*(3), 631-657.

Demirguc-Kunt, A., Lokshin, M., & Torre, I. (2020). The sooner, the better: The early economic impact of non-pharmaceutical interventions during the COVID-19 pandemic. *World Bank Policy Research Working Paper*(9257).

Department of Health. (2020). *COVID-19 Confirmed Cases by Industry Sector*. Retrieved from https://doh.wa.gov/sites/default/files/legacy/Documents/1600/coronavirus//OccupationIndustryReport.pdf

Dev, S. M., & Sengupta, R. (2020). Covid-19: Impact on the Indian economy. *Indira Gandhi Institute of Development Research, Mumbai April*.

Dickens, B. L., Koo, J. R., Lim, J. T., Sun, H., Clapham, H. E., Wilder-Smith, A., & Cook, A. R. (2020). Strategies at points of entry to reduce importation risk of COVID-19 cases and reopen travel. *Journal of travel medicine, 27*(8), taaa141.

Ehlert, A. (2021). The socio-economic determinants of COVID-19: A spatial analysis of German county level data. *Socio-Economic Planning Sciences, 78*, 101083.

Fairlie, R., & Fossen, F. M. (2021). The early impacts of the COVID-19 pandemic on business sales. *Small Business Economics*, 1-12.

Fana, M., Torrejón Pérez, S., & Fernández-Macías, E. (2020). Employment impact of Covid-19 crisis: from short term effects to long terms prospects. *Journal of Industrial and Business Economics, 47*(3), 391-410.

Fernandes, N. (2020). Economic effects of coronavirus outbreak (COVID-19) on the world economy. *Available at SSRN 3557504*.

Fernández-Villaverde, J., & Jones, C. I. (2020). *Estimating and simulating a SIRD model of COVID-19 for many countries, states, and cities* (0898-2937). Retrieved from

Galbusera, L., & Giannopoulos, G. (2018). On input-output economic models in disaster impact assessment. *International journal of disaster risk reduction, 30*, 186-198.

Gros, C., & Gros, D. (2021). The economics of stop-and-go epidemic control. *Socio-Economic Planning Sciences*, 101196.

Gupta, S., Simon, K. I., & Wing, C. (2020). Mandated and voluntary social distancing during the covid-19 epidemic: A review.

Hartikainen, M., Miettinen, K., & Wiecek, M. M. (2012). PAINT: Pareto front interpolation for nonlinear multiobjective optimization. *Computational optimization and applications, 52*(3), 845-867.

Hevia, C., & Neumeyer, A. (2020). A conceptual framework for analyzing the economic impact of COVID-19 and its policy implications. *UNDP LAC COVID-19 Policy Documents Series, 1*, 29.

Hishikar, S. (2021). Assessing the Impact of COVID-19 First Wave on Indian Economy Using Inoperability Input-Output Approach. *Available at SSRN 3910343*.

Hu, Y. (2020). Intersecting ethnic and native–migrant inequalities in the economic impact of the COVID-19 pandemic in the UK. *Research in Social Stratification and Mobility, 68*, 100528.

Hwang, C.-L., & Masud, A. S. M. (2012). *Multiple objective decision making—methods and applications: a state-of-the-art survey* (Vol. 164): Springer Science & Business Media.

Inoue, H., & Todo, Y. (2020). The propagation of economic impacts through supply chains: The case of a mega-city lockdown to prevent the spread of COVID-19. *PloS one, 15*(9), e0239251.

Iri, M. (1971). On an extension of the maximum-flow minimum-cut theorem to multicommodity flows. *Journal of the Operations Research Society of Japan, 13*(3), 129-135.

Isard, W., Azis, I. J., Drennan, M. P., Miller, R. E., Saltzman, S., & Thorbecke, E. (2017). *Methods of interregional and regional analysis*: Taylor & Francis.

Jackson, J. K., Weiss, M. A., Schwarzenberg, A. B., & Nelson, R. M. (2020). Global economic effects of COVID-19.

Janiak, A., Machado, C., & Turén, J. (2021). Covid-19 contagion, economic activity and business reopening protocols. *Journal of economic behavior & organization, 182*, 264-284.

Kermack, W. O., & McKendrick, A. G. (1927). A contribution to the mathematical theory of epidemics. *Proceedings of the royal society of london. Series A, Containing papers of a mathematical and physical character, 115*(772), 700-721.

Lee, W., Liu, S., Tembine, H., Li, W., & Osher, S. (2021). Controlling propagation of epidemics via mean-field control. *SIAM Journal on Applied Mathematics, 81*(1), 190-207.

Leontief, W. (1986). *Input-output economics*: Oxford University Press.

Leung, M., Haimes, Y. Y., & Santos, J. R. (2007). Supply-and output-side extensions to the inoperability input-output model for interdependent infrastructures. *Journal of Infrastructure Systems, 13*(4), 299-310.

Li, B., Barker, K., & Sansavini, G. (2017). Measuring community and multi-industry impacts of cascading failures in power systems. *IEEE Systems Journal, 12*(4), 3585-3596.

Maliszewska, M., Mattoo, A., & Van Der Mensbrugghe, D. (2020). The potential impact of COVID-19 on GDP and trade: A preliminary assessment. *World Bank Policy Research Working Paper*(9211).

Martins-Filho, P., Quintans-Júnior, L., de Souza Araújo, A., Sposato, K., Tavares, C. S., Gurgel, R., . . . Santos, V. (2021). Socio-economic inequalities and COVID-19 incidence and mortality in Brazilian children: a nationwide register-based study. *Public Health, 190*, 4-6.

Mavrotas, G., & Florios, K. (2013). An improved version of the augmented ε-constraint method (AUGMECON2) for finding the exact pareto set in multi-objective integer programming problems. *Applied mathematics and computation, 219*(18), 9652-9669.

McKibbin, W., & Fernando, R. (2020). The economic impact of COVID-19. *Economics in the Time of COVID-19, 45*.

Miller, R. E., & Blair, P. D. (2009). *Input-output analysis: foundations and extensions*: Cambridge university press.

Naimoli, A. (2022). Modelling the persistence of Covid-19 positivity rate in Italy. *Socio-Economic Planning Sciences*, 101225.

Newdick, C., Sheehan, M., & Dunn, M. (2020). Tragic choices in intensive care during the COVID-19 pandemic: on fairness, consistency and community. *Journal of Medical Ethics, 46*(10), 646-651.

Nicola, M., Alsafi, Z., Sohrabi, C., Kerwan, A., Al-Jabir, A., Iosifidis, C., . . . Agha, R. (2020). The socio-economic implications of the coronavirus and COVID-19 pandemic: a review. *International journal of surgery*.

Ocampo, L., & Yamagishi, K. (2020). Modeling the lockdown relaxation protocols of the Philippine government in response to the COVID-19 pandemic: An intuitionistic fuzzy DEMATEL analysis. *Socio-Economic Planning Sciences, 72*, 100911.

Organization, W. H. (2020). *Transmission of SARS-CoV-2: implications for infection prevention precautions: scientific brief, 09 July 2020*. Retrieved from

Panovska-Griffiths, J., Kerr, C. C., Stuart, R. M., Mistry, D., Klein, D. J., Viner, R. M., & Bonell, C. (2020). Determining the optimal strategy for reopening schools, the impact of test and trace interventions, and the risk of occurrence of a second COVID-19 epidemic wave in the UK: a modelling study. *The Lancet Child & Adolescent Health, 4*(11), 817-827.

Paton, A. (2020). Fairness, ethnicity, and COVID-19 ethics. *Journal of Bioethical Inquiry, 17*(4), 595-600.

Pichler, A., & Farmer, J. D. (2021). Simultaneous supply and demand constraints in input–output networks: the case of Covid-19 in Germany, Italy, and Spain. *Economic Systems Research*, 1-21.

Principato, L., Secondi, L., Cicatiello, C., & Mattia, G. (2020). Caring more about food: The unexpected positive effect of the Covid-19 lockdown on household food management and waste. *Socio-Economic Planning Sciences*, 100953.

Pronk, N. P., & Kassler, W. J. (2020). Balancing health and economic factors when reopening business in the age of COVID-19. *Journal of occupational and environmental medicine, 62*(9), e540-e541.

Rahman, A. A., Jasmin, A. F., & Schmillen, A. (2020). *The Vulnerability of Jobs to COVID-19: The Case of Malaysia*: ISEAS-Yusof Ishak Institute.

Richiardi, M., Bronka, P., & Collado, D. (2020). The economic consequences of COVID-19 lockdown in the UK. an input-output analysis using consensus scenarios. *Journal of Chemical Information and Modeling, 53*(9), 1689-1699.

Routley, N. (2020). Charts: The economic impact of COVID-19 in the US so far. *Visual Capitalist*.

Saidan, M. N., Shbool, M. A., Arabeyyat, O. S., Al-Shihabi, S. T., Al Abdallat, Y., Barghash, M. A., & Saidan, H. (2020). Estimation of the probable outbreak size of novel coronavirus (COVID-19) in social gathering events and industrial activities. *International Journal of Infectious Diseases, 98*, 321-327.

Santos, J. R. (2006). Inoperability input-output modeling of disruptions to interdependent economic systems. *Systems Engineering, 9*(1), 20-34.

Sarmidi, T., Khalid, N., Zainuddin, M. R. K., & Jusoh, S. (2021). The COVID-19 Pandemic, Air Transport Perturbation, and Sector Impacts in ASEAN Plus Five: A Multiregional Input–Output Inoperability Analysis.

Seyedin, H., Zanganeh, A.-M., Mojtabaei, M., Bagherzadeh, R., & Faghihi, H. (2020). A model of reopening businesses to decrease the heath and economic impacts of the COVID-19 pandemic: Lessons from Iran. *Medical journal of the Islamic Republic of Iran, 34*, 97.

Socci, C., Ahmed, I., Alfify, M. H., Deriu, S., Ciaschini, C., & Sheikh, R. A. (2021). COVID-19 and a trade-off between health and economics: an extended inoperability model for Italy. *Kybernetes*.

Soufi, H. R., Esfahanipour, A., & Shirazi, M. A. (2022). A quantitative approach for analysis of macroeconomic resilience due to socio-economic shocks. *Socio-Economic Planning Sciences, 79*, 101101.

Stevenson, B. (2020). The initial impact of COVID-19 on labor market outcomes across groups and the potential for permanent scarring. *The Hamilton Project*.

Sumner, A., Hoy, C., & Ortiz-Juarez, E. (2020). *Estimates of the Impact of COVID-19 on Global Poverty*: United Nations University World Institute for Development Economics Research.

Surgo Ventures. (2021a). Report: Vulnerable Communities and COVID-19. Retrieved from https://precisionforcovid.org/ccvi. Retrieved 2022 https://precisionforcovid.org/ccvi

Surgo Ventures. (2021b). *Vulnerable Communities and COVID-19: The Damage Done, and the Way Forward*. Retrieved from Surgo Ventures, : https://surgoventures.org/resource-library/report-vulnerable-communities-and-covid-19

Suryahadi, A., Al Izzati, R., & Suryadarma, D. (2020). Estimating the impact of covid-19 on poverty in Indonesia. *Bulletin of Indonesian Economic Studies, 56*(2), 175-192.

University of Maryland. (2020). COVID-19 Impact Analysis Platform. Retrieved from https://data.covid.umd.edu/. Retrieved January 2022 https://data.covid.umd.edu/

Wang, L., Wang, F., Zhou, Y., & Song, P. X. (2020). Discussion of" Tracking reproductivity of COVID-19 epidemic in China with varying coefficient SIR model". *Journal of Data Science, 18*(3), 477-479.

White, D. B., & Angus, D. C. (2020). A proposed lottery system to allocate scarce COVID-19 medications: promoting fairness and generating knowledge. *Jama, 324*(4), 329-330.

Yu, K. D. S., & Aviso, K. B. (2020). Modelling the economic impact and ripple effects of disease outbreaks. *Process Integration and Optimization for Sustainability, 4*(2), 183-186.

Yu, K. D. S., Aviso, K. B., Santos, J. R., & Tan, R. R. (2020). The economic impact of lockdowns: A persistent inoperability input-output approach. *Economies, 8*(4), 109.

Zhou, L., Wu, K., Liu, H., Gao, Y., & Gao, X. (2020). CIRD-F: Spread and Influence of COVID-19 in China. *Journal of Shanghai Jiaotong University (Science), 25*(2), 147-156.

Zhu, P., Wang, X., Li, S., Guo, Y., & Wang, Z. (2019). Investigation of epidemic spreading process on multiplex networks by incorporating fatal properties. *Applied mathematics and computation, 359*, 512-524.

Zimmermann, M., Benefield, A. E., & Althouse, B. M. (2020). They stumble that run fast: the economic and COVID-19 transmission impacts of reopening industries in the US. *medRxiv*.